

LAND SURFACE TEMPERATURE RETRIEVAL FROM LANDSAT-8

A DISSERTATION

SUBMITTED IN THE PARTIAL FULFILLMENT OF THE REQUIREMENTS

FOR

THE AWARD OF THE DEGREE

OF

MASTER OF TECHNOLOGY

IN

SOFTWARE ENGINEERING

Submitted by:

Anshul Verma (2K20/SWE/04)

Under the supervision of

DR. ABHILASHA SHARMA



DEPARTMENT OF SOFTWARE ENGINEERING

DELHI TECHNOLOGICAL UNIVERSITY

(Formerly Delhi College of Engineering)

Bawana Road, Delhi-110042

MAY 2022

M.TECH (Software Engineering)

Anshul Verma 2022

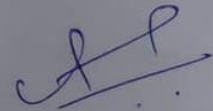
DELHI TECHNOLOGICAL UNIVERSITY
(Formerly Delhi College of Engineering)
Bawana Road, Delhi- 110042

CANDIDATE'S DECLARATION

I, Anshul Verma (2K20/SWE/04) of MTech (Software Engineering), hereby declare that the project dissertation titled " **Land Surface Temperature Retrieval from Landsat-8**" submitted by me to the Department of Software Engineering, Delhi Technological University, Delhi in partial fulfilment of the requirement for the award of the degree of Master of Technology, is original and not copied from any source without proper citation. This work has not previously formed the basis for the award of any degree, diploma associateship, fellowship or other similar title or recognition

Place: Delhi

Date: 30/5/22



ANSHUL VERMA

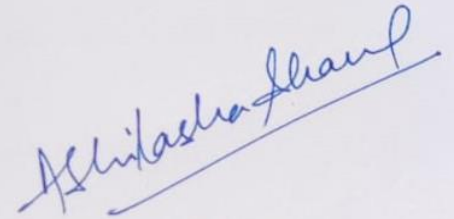
DELHI TECHNOLOGICAL UNIVERSITY
(Formerly Delhi College of Engineering)
Bawana Road, Delhi- 110042

CERTIFICATE

This is to certify that this project dissertation entitled " **Land Surface Temperature Retrieval from Landsat-8**" submitted by Anshul Verma(2K20/SWE/04) Department of Software Engineering, Delhi Technological University, Delhi, in partial fulfilment of the requirement for the award of the degree of Master of Technology, is a record of the original work carried out by him under my supervision.

Place: Delhi

Date: 30/5/22



DR. ABHILASHA SHARMA

SUPERVISOR

Assistant Professor,
Department of Software Engineering,
Delhi Technological University,
(Formerly Delhi College of Engineering),
Shahbad Daulatpur,
Main Bawana Road, Delhi-110042.

ACKNOWLEDGMENT

The success of this project requires the assistance and input of numerous people and the organization. I am grateful to everyone who helped in shaping the result of the project.

I express my sincere thanks to **Dr. Abhilasha Sharma**, my project guide, for providing me with the opportunity to undertake this project under her guidance. Her constant support and encouragement have made me realize that it is the process of learning which weighs more than the result. I am highly indebted to the panel faculties during all the progress evaluations for her guidance, constant supervision and for motivating me to complete my work. She helped me throughout with innovative ideas, provided information necessary and pushed me to complete the work.

I also thank all my fellow students and my family for their continued support.

ANSHUL VERMA

ABSTRACT

Land surface temperature, or LST, is the temperature of a surface that may be measured when it is in direct contact with a measuring equipment. It is known as the radiative skin temperature of land, and it is obtained from infrared radiation. The "skin" temperature is the temperature of the top surface when it is on bare soil, and the temperature of plant "canopies" is defined by the top of the canopy for effective emitting.

At simple terms, LST may be described as how hot the "surface" of the earth feels when touched in a certain area. However, from a satellite's perspective, "surface" is what it sees while looking through the atmosphere to the earth. The view might be from a structure, a body of water, or any geographical or manmade surface.

In this research work attempt has been made to study the temporal and spatial variation of Land surface Temperature in the northern part of India that mainly focuses on Varanasi region from May 2013 to May 2021 using Landsat 8 - OLI & TIRS satellite dataset. The variation in Land surface temperature with the various Land use and cover classes have been also analyzed this research-work aims on forming an ERDAS imagine model for retrieving the Land surface temperature (LST) with the help of Landsat 8 thermal images and metadata of band 10 data. The correlation of Land Surface Temperature (LST) with Normalized Difference Vegetation Index (NDVI) and Normalized Difference Built-up Index (NDBI) is also studied and discussed in the thesis. The result shows that LST shares a positive relationship with the NDBI but a negative relationship with the NDVI. The built-up area (urbanization) for the area of interest in 2013 was 121.7 km² which significantly increased

to 200.38 km² in 2021. Hence, the total increase in the built-up area from 2013 to 2021 (8-year time-period) is 8.62% of the total land cover that is 913.48 km². After analysing the variation of LST with different LULC classes, it was evident that the spike in the Land surface temperature in the area of interest was caused because there has been increase in impervious area which not only increase the built-up area but also decreases per capita tree cover of the region

TABLE OF CONTENTS

| | |
|--|-----|
| CANDIDATE’S DECLARATION..... | ii |
| CERTIFICATE..... | iii |
| ACKNOWLEDGEMENT..... | iv |
| ABSTRACT..... | v |
| TABLE OF CONTENT..... | vii |
| LIST OF FIGURE(s)..... | ix |
| LIST OF TABLES(s)..... | xi |
| LIST OF ABBREVIATION(s)..... | xii |
| CHAPTER 1 INTRODUCTION..... | 1 |
| 1.1: Land Surface Temperature..... | 1 |
| 1.2: Main Objectives..... | 2 |
| 1.3: Software Used..... | 2 |
| CHAPTER 2 LITERATURE REVIEW..... | 3 |
| CHAPTER 3 STUDY AREA & DATA USED..... | 6 |
| 3.1: Study area..... | 6 |
| 3.2: Data used..... | 7 |
| CHAPTER 4 METHODOLOGY..... | 10 |
| 4.1: Our Approach..... | 10 |
| 4.2: Collection of satellite data..... | 11 |
| 4.3: Pre-processing of images..... | 11 |
| 4.3.1: Layer stacking..... | 11 |

| | |
|--|----|
| 4.3.2: Clipping of the image..... | 12 |
| 4.3.3: Histogram equalization..... | 12 |
| 4.4: LULC classification..... | 12 |
| 4.5: LULC maps..... | 14 |
| 4.6: Land surface temperature retrieval..... | 16 |
| 4.6.1: Conversion of DN to radiance..... | 18 |
| 4.6.2: Brightness temperature..... | 19 |
| 4.6.3: Normalized difference vegetation index (NDVI)-..... | 19 |
| 4.6.4: Normalized difference Built-up index (NDBI)..... | 19 |
| 4.6.5: Proportional vegetation cover..... | 20 |
| 4.6.6: Land surface emissivity..... | 20 |
| 4.6.7: Land surface temperature..... | 21 |
| 4.7: LST variation with different LULC classes..... | 25 |
| 4.8: Correlation analysis..... | 40 |
| CHAPTER 5 RESULTS & DISCUSSION..... | 44 |
| CHAPTER 6 CONCLUSION..... | 47 |
| REFERENCES..... | 48 |

LIST OF FIGURE(S)

| | |
|--|----|
| Figure 3. 1: Location map of study area..... | 7 |
| Figure 3. 2: Landsat 8 band designations for the Operational Land Imager (OLI) and Thermal Infrared Sensor (TIRS)..... | 9 |
| Figure 4. 1: Flowchart of the methodology..... | 10 |
| Figure 4. 2: LULC map of study area 01-05-2013..... | 14 |
| Figure 4. 3: LULC map of study area 12-05-2017..... | 15 |
| Figure 4. 4: LULC map of study area 23-05-2021..... | 16 |
| Figure 4. 5: Flowchart of retrieving LST from Landsat 8 image..... | 18 |
| Figure 4. 6: LST map of study area 01-05-2013..... | 22 |
| Figure 4. 7: LST map of study area 12-05-2017 | 23 |
| Figure 4. 8: LST map of study area 23-05-2021..... | 24 |
| Figure 4. 9: Variation of LST with Built-up 01-05-2013..... | 25 |
| Figure 4. 10: Variation of LST with Built-up 12-05-2017..... | 26 |
| Figure 4. 11: Variation of LST with Built-up 23-05-2021..... | 27 |
| Figure 4. 12: Variation of LST with Fallow land 01-05-2013..... | 28 |
| Figure 4. 13: Variation of LST with Fallow land 12-05-2017..... | 29 |
| Figure 4. 14: Variation of LST with Fallow land 23-05-2021..... | 30 |
| Figure 4. 15: Variation of LST with Vegetation 01-05-2013 | 31 |
| Figure 4. 16: Variation of LST with Vegetation 12-05-2017 | 32 |
| Figure 4. 17: Variation of LST with Vegetation 23-05-2021..... | 33 |
| Figure 4. 18: Variation of LST with Waterbody 01-05-2013 | 34 |
| Figure 4. 19: Variation of LST with Waterbody 12-05-2017 | 35 |
| Figure 4. 20: Variation of LST with Waterbody 23-05-2021..... | 36 |
| Figure 4. 21: Variation of LST with Sand 01-05-2013..... | 37 |
| Figure 4. 22: Variation of LST with Sand 12-05-2017..... | 38 |
| Figure 4. 23: Variation of LST with Sand 23-05-2021..... | 39 |
| Figure 4. 24: Trend analysis of LST with NDVI 01-05-2013..... | 40 |

| | |
|--|----|
| Figure 4. 25: Trend analysis of LST with NDBI 01-05-2013 | 41 |
| Figure 4. 26: Trend analysis of LST with NDVI 12-05-2017..... | 41 |
| Figure 4. 27: Trend analysis of LST with NDBI 12-05-2017 | 42 |
| Figure 4. 28: Trend analysis of LST with NDVI 23-05-2021..... | 42 |
| Figure 4. 29: Trend analysis of LST with NDBI 23-05-2021..... | 43 |

LIST OF TABLE(S)

| | |
|---|----|
| Table 3 1: Details of the satellite data collected..... | 8 |
| Table 4 1: Classification Accuracy statistics..... | 14 |
| Table 4 2: Rescaling factor..... | 17 |
| Table 4 3: K1 and K2 values..... | 17 |
| Table 5. 1: LULC classes and their areas in different years..... | 44 |
| Table 5. 2: LST values retrieved from different Landsat 8 images..... | 45 |
| Table 5. 3: LULC classes and their LST values..... | 46 |

LIST OF ABBREVIATION(S)

| Abbreviations | Full forms |
|----------------------|--|
| LST | Land Surface Temperature |
| OLI | Operational Land Imager |
| TIRS | Thermal Infrared Sensor |
| ERDAS | Earth Resource Data Analysis System |
| NDVI | Normalize Difference Vegetation Index |
| NDBI | Normalize Difference Built-up Index |
| LULC | Land Use Land Cover |
| USGS | United State Geological Survey |
| AOI | Area of Interest |
| LANDSAT | Land Remote Sensing Satellite |
| NASA | National Aeronautical and Space Administration |

CHAPTER 1

INTRODUCTION

1.1: Land Surface Temperature

Land surface temperature, or LST, measures temperature on a surface that is observed when it is in direct connection with a equipment or sensor that measures temperature. It is known as the radiative skin temperature of land, and it is obtained from infrared radiation. The "skin" temperature will be observed temperature at the top surface when on bare soil, and the temperature of plant "canopies" is defined by the top of the canopy for effective emitting.

At simple terms, LST may be described as how hot the "surface" of the earth feels when touched in a certain area. However, from a satellite's perspective, "surface" is what it sees while looking through the atmosphere to the earth. The view might be from a structure, a body of water, or any geographical or manmade surface.

The temperature of a ground that can be measured when it comes into direct contact with measurement equipment is known as land surface temperature, or LST. It is derived from infrared radiation and is recognized as the radiative surface temperatures of land. The temperature of plant "canopies" is described by the top of the canopy for efficient emission, while the temperature of "skin" is the temperature of the upper surface when it is on bare soil.

LST may be defined as to how warm the "surface" of the earth seems when touched in a certain place. However, "surface" refers to what a satellite observes while peering through the earth. The view could be from a building or a body of water.

LST, is the temperature of the ground that may determine when it comes into contact with measuring equipment. It is known as the radiative surface temperatures of ground and is obtained from infrared radiation. The temperature of plant "canopies" is characterized by the top of the canopy for effective emission, but the temperature of "skin" is the temperature of the top surface when it is on bare soil. LST may be described as how warm the earth's "surface" seems when felt in a certain location. Instead, "surface" refers to how a satellite sees through the earth's atmosphere. It might be a view from a structure or a body of water.

Anthropogenic and natural activities influence an area's land use and land cover, which in turn influences the land surface temperature, as if the area has a high percentage of built-up area and a low proportion of vegetative cover, the LST will rise, and if the area has a high proportion of vegetative cover, the LST will fall.

LST fluctuates geographically owing to land surface cover heterogeneity, environmental temperature and humidity fluctuations, clouds and big particles in the air such as dust, and other meteorological phenomena.

LST is an interesting phenomenon to explore since it exhibits both temporal and geographical variability. The LST has been determined by several academics and scholars using various methodologies and algorithms. It was extremely difficult to determine an area's LST prior to the development of remote sensing satellites (EOS). It was often generated manually by choosing several ground control locations within the research area using temperature measurement devices, and these data were then converted into isotherms . LST may now be determined geographically thanks to the development of satellites and high-resolution sensors. It may be estimated for any area on the planet using thermal infrared bands provided by satellites.

Some of the satellites/sensors which can be used for calculation of LST are, ASTER, Landsat 8 OLI/TIRS, Landsat 7 ETM+, Sentinel-3A/SLSTR, and MODIS Terra satellites.

1.2: Main Objective

The primary aim of this study are as follows:

- 1) To study the variation of Land Surface Temperature in the Varanasi region from May 2013 to May 2021 by using Landsat 8 data.
- 2) To study the Land Use/Cover variation in area of interest and analyze the variation of Land Surface Temperature with different Land Use/Cover classes.
- 3) Calculation of Normalized Difference Vegetation Index (NDVI) and Normalized Difference Built up Index (NDBI).
- 4) To study the pattern and similarity formation of LST with NDVI and LST with NDBI.

1.3: Software Used

ERDAS IMAGINE 2015 and Esri's ARCGIS 10.8 were utilized in this investigation. ERDAS IMAGINE 2015 can be used for layer stacking, mosaicking, reprojection, and image classification, while IMAGINE MODEL MAKER is utilized to create a model for calculating LST using Landsat8 data.

ARCGIS10.8 is used to examine and edit geographic data as well as create maps. It is also employed in correlation research here between LST and various metrics.

CHAPTER 2

LITERATURE REVIEW

The significance of Land surface temperature (LST) recovered from high and medium spatial and temporal resolution Remotely Sensed data for many environmental science, particularly those related to water resource management over agricultural sites, was a major factor in the final decision to include a thermal infrared (TIR) device onboard the Landsat Data Continuity Mission or Landsat 8. At both the local and global stages, land surface temperature (LST) is an essential metric connected to surface energy and water balance. Several methods for retrieving LST from space-based thermal infrared (TIR) data have been developed.

Land surface temperature has gained importance in recent years, as well as the need to develop methods for determining LST using satellite pictures. TIR sensing remotely, and also passive microwave, may be used to measure land surface temperature. Only under clear skies can LST observed by IR thermal sensors give better spatial resolution. Microwave Remote Sensing has the ability to reduce air pollution since air particles are invisible to microwave frequency at levels near around 12 GHz. Passive microwave sensors, on the other hand, have a reduced spatial resolution and accuracy. Satellite-derived datasets are also utilized for a number of applications such as large-scale ecological stress detection, rainfall monitoring, land surface monitoring, biodiversity research, and the impacts of urban heat islands.

This section discusses several major landmark research papers released on LST using Landsat 8 imagery dataset that were established by researchers over the years on the basis of analytical and experimental analyses.

Rajeshwari A, Mani N D (2014) conducted comprehensive research on the calculation of observed temperature of land using the satellite Landsat 8 dataset of Dindigul district of Tamil Nadu, India. The LST for Dindigul district, Tamil Nadu, India, came to using the Split Window (SW) technique and Landsat 8 OLI/TIRS dataset for this research. To calculate LST, the SW method requires the spectral radiance and emissivity of two TIR

bands as the input. TIR bands 10 and 11 were used to calculate spectral radiance. Emissivity was calculated using the NDVI threshold approach using OLI bands 2, 3, 4, and 5. The study clearly demonstrated that because the area had higher vegetative cover in mountain areas, the LST in the southern part of the district was low and the northern plains, which had barren regions, uncultivated land, and urban centers, had high LST.

Subhanil Guha, Himanshu Gill, Anindita Dey, and Neetu Gill (2018) conducted comprehensive research in Florence and Naples, Italy, on Analytical analysis of LST using NDVI and NDBI that uses the dataset acquired from the Landsat 8 (TIRS and OLI). In this paper, the Landsat 8 datasets have been accustomed to explore the intensity of UHI in the Italian towns of Florence and Naples, as well as to analyze link in LST and NDVI and NDBI. UHI zones were found using LST and scattered in the center region of Florence, from the north-west to the south-east, and developing throughout the eastern half of Naples. LST is mostly generated by land and built-up regions. The presence of plants and bodies of water lessens the Level of LST Several UHS were also defined inside UHI zones that had significant concentrations of LST.

There is a connection among LST–NDVI and LST–NDBI was evaluated at the pixel level using linear regression analysis. LST has a significant negative association (0.71 and 0.57) with NDVI and a significant positive correlation (0.71 and 0.61) with NDBI for whole Florence and Naples cities. For UHI, the relationships deteriorate. It might be because of the existence of more diverse landscapes inside the built-up region.

Gordana Kaplan, Ugur Avdan and Zehra Yigit Avdan (2018) carried out In Skopje, Macedonia, research on Urban Heat Island Analysis Using Landsat 8 Satellite Data: A Case Study was carried out. The influence of UHI is examined in this study utilizing Landsat 8 dataset from 2013–2017 like a research study in Skopje, Macedonia. The distribution of land surface temperature (LST) is collected using Landsat 8 dataset with an algorithm. Furthermore, the pattern in LST and the NDVI and the normalized difference built-up index (NDBI) is observed in order to investigate the influence of green spaces and built-up surface in heat island in urban region. According to it, there is findings, that influence of said urban heat island in Skopje may be found inside numerous sub-urban locations.

There is a negative link with LST and NDVI shows that greener space has reduce impact of the urban heat island, whereas the positive link with LST and NDBI indicates that built-up land increase impact of the urban heat island in studied region. As a result of this research, it is possible to infer that, in order to lessen UHI impacts, local authorities increase quantity of greener region in densely occupied metropolitan regions.

CHAPTER 3

STUDY AREA & DATA USED

3.1: Study Area

Study area for this thesis includes the areas on either side of the bank of river Ganges in Varanasi district (Uttar Pradesh, India). The area includes the majority of Varanasi city and some portion of neighboring district Chandauli (Mughal Sarai) and Mirzapur district of India.

Varanasi city, which is located at the center of Ganges Valley which belongs to the Northern part of India and also the left crescent-shaped bank of the Ganges River. Varanasi has a humid subtropical weather and there is a huge variation with the observed temperature of summer and winter. The observed temperature in area of interest difference between 22°C - 46°C in summer time and in the rainy season its average rainfall is 1110mm. As the area of interest lies in the alluvial plain on the bank of the river Ganges, soil in this region has a good proportion of sand, silt and clay.

The area of interest selected has water, fallow land, vegetation, sand and urban areas (built-up) in good proportions. The study has been conducted to see whether there is any effect of the land use and land cover so that LST can be studied on this area of interest.

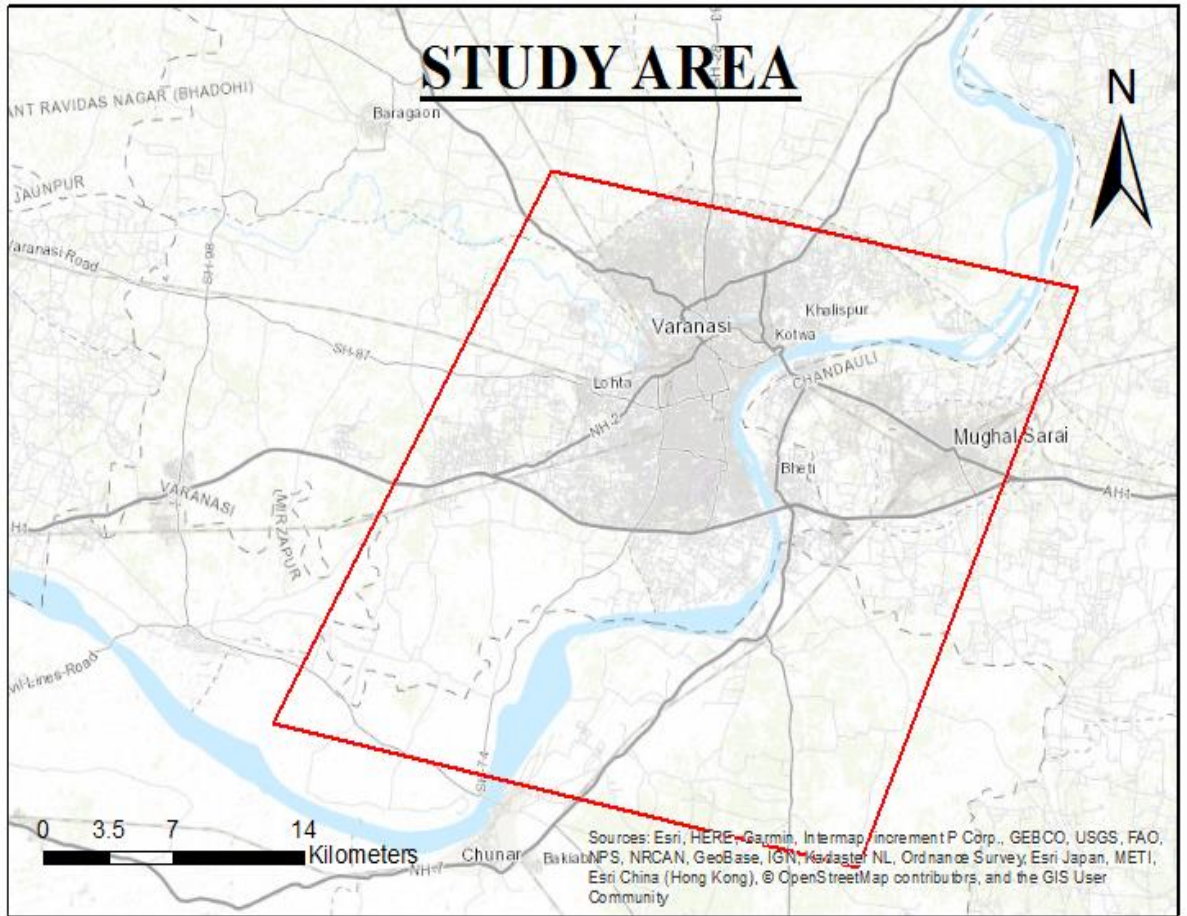


Figure 3. 1: Satellite image of study area

3.2 Data Used

This study uses the data acquired by the LANDSAT 8 satellite which is freely available for public usage inside the archive of USGS which is present on the following website <https://earthexplorer.usgs.gov/>. On earth explorer Landsat 8 satellite images can be seen inside the dropdown menu named as “Landsat” under which there is another option named as “Landsat Collection 1 Level-1”, finally we will select “Landsat8 OLI/TIRS C1 Level-1” images dataset along with its metadata files for our research work

The Landsat 8 is a satellite made in America used for observation of Earth it was made under the LANDSAT program on 11 February 2013 and is the seventh version in the bundle of satellites that is successfully remote sensing the earth surface. It was jointly made by NASA and USGS (United States Geological Survey), launch vehicle and the

mission critical system were made by NASA and USGS provided with the remote sensing devices, under the remote sensing devices the 2 main devices are:

1. Operational Land Imager - It is an instrument that is used for remote sensing used in all LANDSAT satellite versions, basically it is a telescope and works along with TIRS to collect different band that captures images that are used for purpose
2. Thermal Infrared sensor- It is a sensor which study the temperature of the surface on the Earth.

The satellite captures the data of the Earth in a cycle which has a time period of 16 days. OLI captures the images and its related data; its resolution can be up to 30 meters it has 8 bands where Band 1 is used capture water bodies at shallow level and it can track the aerosols. Band 2,3 and 4 is used to capture the images in visible wavelength spectrum and can form a true color image. Band 5 is for ecological areas; 6&7 are used to differentiate between soil and rock and also a panchromatic band which has a 15-meter resolution spatially. TIRS is used to read the thermal infrared radiance with a 100-meter resolution and it uses 2 bands which resides inside the window of the atmosphere that is present in between 10 and 12 micrometers. The designation of bands of Landsat 8 are shown in the figure 3.2

TIRS sensor observes thermal infrared radiance with a resolution of 100 meter with band 10 and band 11 which is present on the window of atmosphere in between 10 and 12 micrometers. Designation of the band in the Landsat 8 can be shown in **Figure 3.2**.

The remote images captured by the satellite are of multispectral form, hence the images through USGS website of Varanasi region are collected for 3 different dates. The satellite data collected represented with the **Table 3.1**.

Table 3.1 – Shows the data collected from the satellite

| Year | Acquired data date | Used Sensors | Path/row | Cloud cover |
|------|--------------------|--------------------|----------|-------------|
| 2013 | 01-05-2013 | Landsat 8 OLI/TIRS | 142 /43 | 0.0% |
| 2017 | 12-05-2017 | Landsat 8 OLI/TIRS | 142/43 | 0.03% |
| 2020 | 23-05-2021 | Landsat 8 OLI/TIRS | 142/43 | 0.03% |

| Landsat 8 Operational Land Imager (OLI) and Thermal Infrared Sensor (TIRS) Launched February 11, 2013 | Bands | Wavelength (micrometers) | Resolution (meters) |
|---|--|-------------------------------------|--------------------------------|
| | Band 1 - Coastal aerosol | 0.43 - 0.45 | 30 |
| | Band 2 - Blue | 0.45 - 0.51 | 30 |
| | Band 3 - Green | 0.53 - 0.59 | 30 |
| | Band 4 - Red | 0.64 - 0.67 | 30 |
| | Band 5 - Near Infrared (NIR) | 0.85 - 0.88 | 30 |
| | Band 6 - SWIR 1 | 1.57 - 1.65 | 30 |
| | Band 7 - SWIR 2 | 2.11 - 2.29 | 30 |
| | Band 8 - Panchromatic | 0.50 - 0.68 | 15 |
| | Band 9 - Cirrus | 1.36 - 1.38 | 30 |
| | Band 10 - Thermal Infrared (TIRS) 1 | 10.60 - 11.19 | 100 |
| Band 11 - Thermal Infrared (TIRS) 2 | 11.50 - 12.51 | 100 | |

Figure 3.2 Band designations of the LANDSAT 8 for the OLI and TIRS

CHAPTER 4

METHODOLOGY

4.1: Our Approach

This report uses the data collected from LANDSAT 8 satellite. In this study a software-based approach is followed to retrieve the LST and also the land usage land covered classification, the software used in this report is ERDAS Imagine 2015. The methodology used in this study is explained with the help of a flowchart given below.

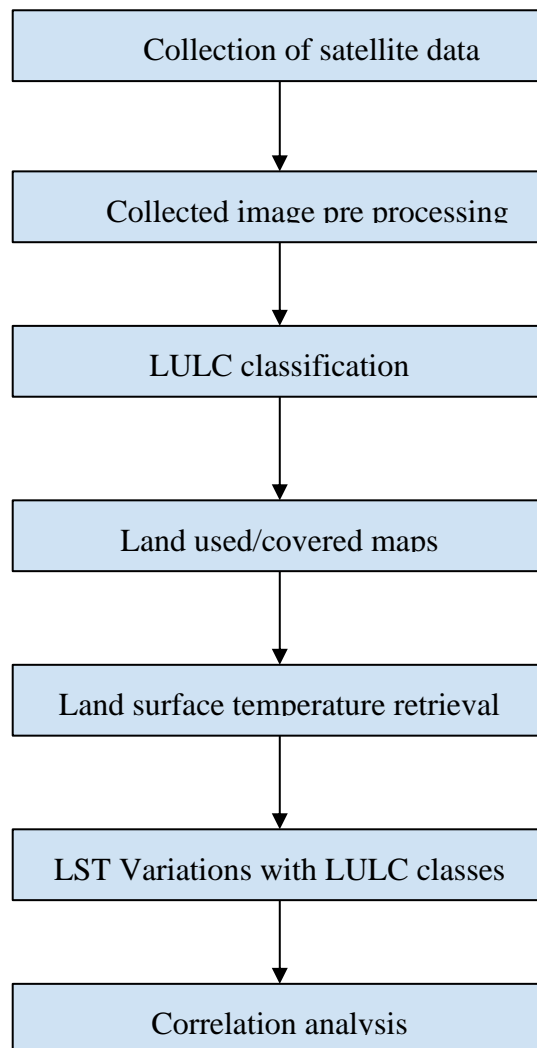


Figure 4. 1: Flowchart of the methodology

4.2: Collection of satellite data

Landsat 8 Multi spectral remote sensing images of the Varanasi region have been collected from USGS. The data collected from the satellite is given in **Table 3.1**.

4.3: Pre-Processing of Images

Preprocessing of images is done using multiple software that deploy various pre-processing functions to remove or suppress the data which not relevant, it also supports or enhances the features that important and relevant for the study. Preprocessing of the images is term that means to enhance the quality of an image using various operations on it while applying minimum level of abstraction. But these functions can not make or increase the information attached with the image, what they can do is to decrease the irrelevant information if entropy is a measure for information. The main focus of preprocessing is to increase image quality using computer algorithms which helps the researcher to analyses it in a better way, it removes the distortion in the image and only enhance the features that a researcher requires for performing the experiment, the features that are enhanced depends upon the application. Preprocessing operations used in this study are as follows:

4.3.1: Layer stacking

Layer stacking as the name suggest is process which is used to combine multiple images into a single image usually single bands with the same spatial resolution are stacked together. After collecting the sufficient amount of satellite images, they are classified in different bands, this activity conducted as soon as the user gets the images and it is one of the primary processes. It is important that all the images should have same spatial resolution so that layer stacking can be performed if the images differ we have resample the images so that it can identical to the target resolution. This process increases the size of the final images which will also increase the processing time if any computation is being performed on it. Some times its better not to stack images so that the whole process can become economical and swift.

4.3.2: Clipping of the image

In clipping process, a subset is created from the raster dataset. In this process the user can remove data irrelevant data from the area of interest which in return decreases the size of the file and also decreases the computing time of many operations that are applied on the images. It allows focus on relevant parts of an image. It is done with the help of a shape file or an AOI (Area of Interest) file

4.3.3: Histogram equalization

Histogram equalization is a technique for preprocessing an image which enhance or adjust the contrast of an image by using the histogram. It can increase or decrease the contrast of an image; it is a widely used image preprocessing technique and is well-known for its efficiency and sophisticated technique. The technique is used for varying the contrast and dynamic range of the images, the shape of histogram changes when the user alters any parameter of the image which in return help to set histogram shape according to the target or desired result

4.4: LULC Classification

LULC classification is a technique of which assign the classes of land cover into pixels which differentiate it this phenomenon is called LULC classification. Sources of Water, metropolis, land for plant growing and farming, activities like cattle domestication and feeding, structures, forests, agriculture, peaks, and concrete structures are only a few examples [2,7].

Land use and land cover patterns influence the fluctuation of surface temperature, as LST exhibits both geographical and temporal variability with changes in land use and land cover patterns. Landsat 8 satellite photos classified for the periods 01-05-2013, 12-05-2017, and 23-05-2021 were used to create LULC maps. ERDAS IMAGINE 2015 program has been used to classify the photos. The classification of images was done using supervised classification with a maximum likelihood classifier.

Built-up area, flora, bodies of water, sand, and fallow land are the 5 major LULC classifications found and defined in this study. Accuracy evaluation was carried out to see how successfully the classification methods were carried out and to learn how to evaluate the classification's usefulness. The error matrix and Kappa coefficient are now widely used to measure picture categorization accuracy. Furthermore, the error matrix

has been employed in many land categorization studies and was an important part of this study. The accuracy level of the classified image depicts how each pixel is categorized in comparison to the Definite land use / cover conditions derived from the ground truth data. The accuracy of the producer is a measure of how effectively real-world land cover categories may be categorized based on mistakes of omission. The error of omission, that quantifies the chance of a categorized pixel matches the land surface type of its associated real-world location, is measured by the user's accuracy

Land use and land cover patterns influence the fluctuation of surface temperature, as LST exhibits both geographical and temporal variability with changes in land use and land cover patterns. Landsat 8 satellite photos classified for the periods 01-05-2013, 12-05-2017, and 23-05-2021 were used to create LULC maps. ERDAS IMAGINE 2015 program has been used to classify the photos.

This study uses the data acquired by the LANDSAT 8 satellite which is freely available for public usage inside the archive of USGS which is present on the following website <https://earthexplorer.usgs.gov/> .On earth explorer Landsat 8 satellite images can be seen inside the dropdown menu named as “Landsat” under which there is another option named as “Landsat Collection 1 Level-1”, finally we will select “Landsat8 OLI/TIRS C1 Level-1” images dataset along with its metadata files for our research work

The classification of images was done using supervised classification with a maximum likelihood classifier. Built-up area, flora, bodies of water, sand, and fallow land are the 5 major LULC classifications found and defined in this study. Accuracy evaluation was carried out to see how successfully the classification methods were carried out and to learn how to evaluate the classification's usefulness. The error matrix and Kappa coefficient are now widely used to measure picture categorization accuracy.

Furthermore, the error matrix has been employed in many land categorization studies and was an important part of this study. The accuracy level of the classified image depicts how each pixel is categorized in comparison to the Definite land use / cover conditions derived from the ground truth data. The accuracy of the producer is a measure of how effectively real-world land cover categories may be categorized based on mistakes of omission. The error of omission, that quantifies the chance of a categorized pixel matches the land surface type of its associated real-world location, is measured by the user's accuracy. Table 4.1 shows the results of accuracy assessments of categorized photos from different years.

Table 4 1: Classification Accuracy statistics

| Date | Overall accuracy (%) | Kappa statistics |
|------------|----------------------|------------------|
| 01-05-2013 | 92.31 | 0.9037 |
| 12-05-2017 | 92.50 | 0.9063 |
| 23-05-2013 | 95.00 | 0.9375 |

4.5: LULC maps

LULC maps for the study area are as follows

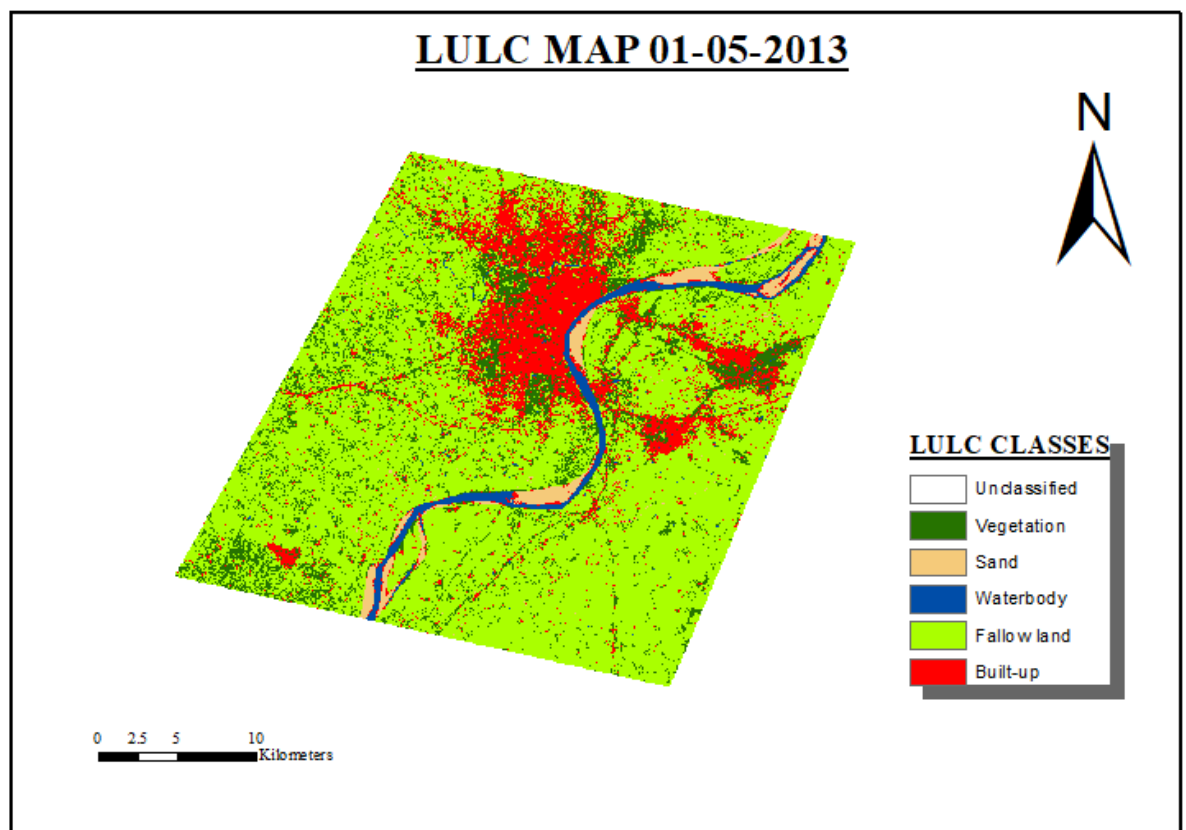


Figure 4. 2: LULC map of study area 01-05-2013

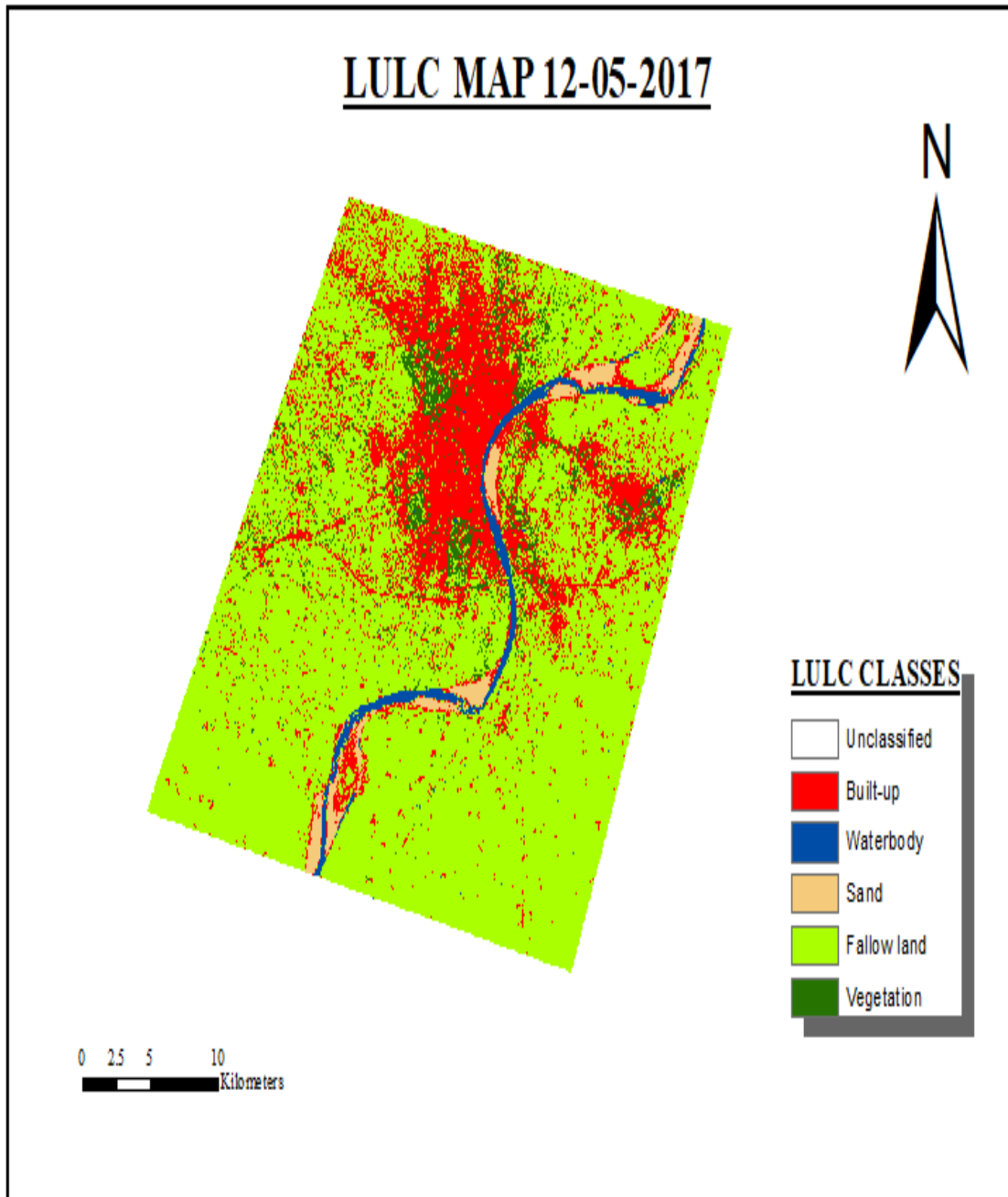


Figure 4. 3: LULC map of study area 12-05-2017

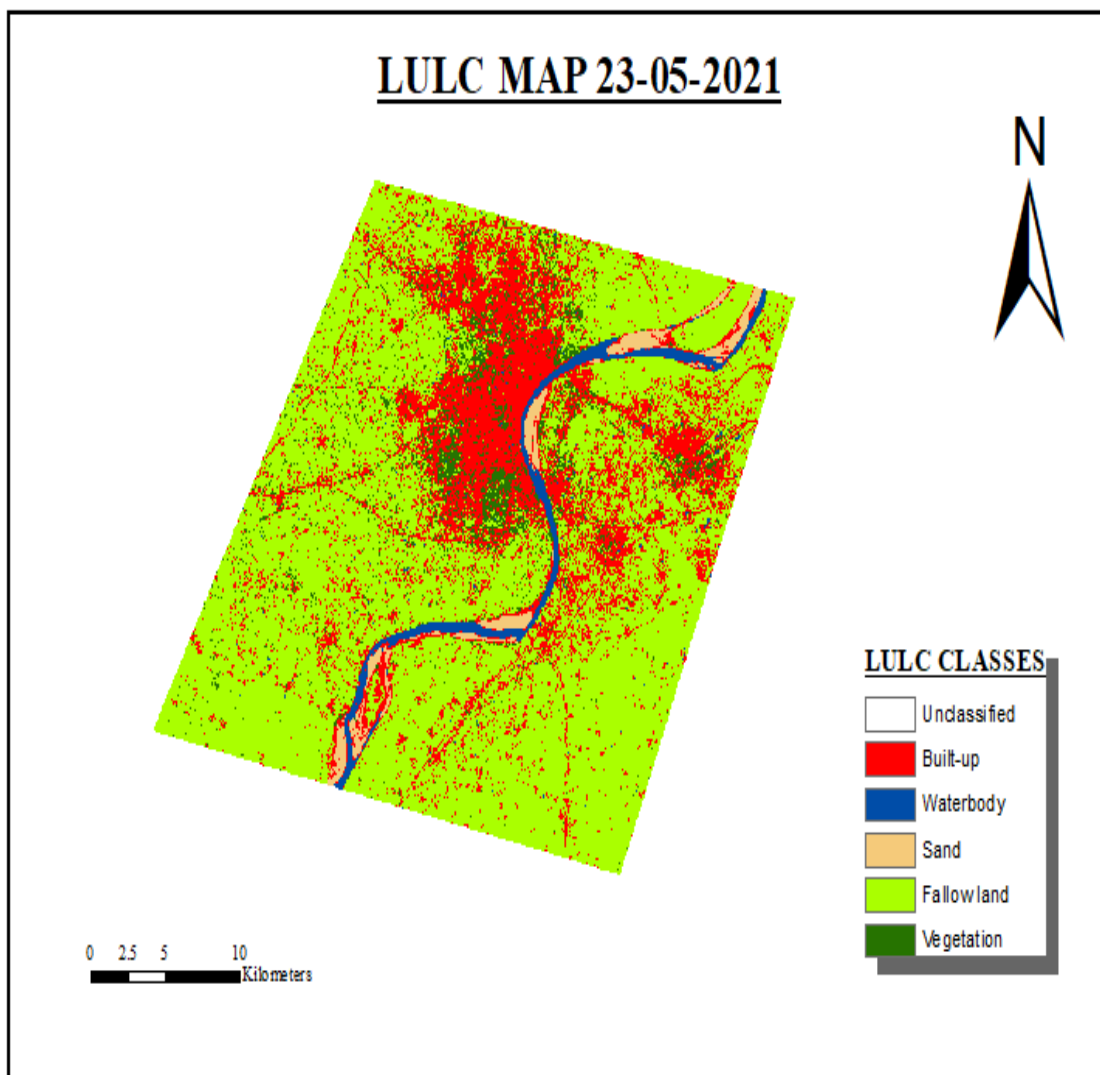


Figure 4. 4: LULC map of study area 23-05-2021

4.6: Land Surface Temperature Retrieval

Landsat 8 data was used to determine the land surface temperature across the Varanasi region. The LST estimation algorithm was designed in ERDAS IMAGINE MODEL MAKER 2015, and this model can only be utilised with Landsat 8 data. TIR band 10 was utilised to measure the brightness temperature in this investigation, while bands 4 and 5 were used to compute the NDVI. The TIR band 11 was not applied to evaluate the brightness temperature because, due to the higher calibration error associated with band

11, the USGS advises users not to depend on band 11 data in quantitative research of TIRS data, such as extraction of surface temperature values. The metadata of satellite images used in the algorithm is presented in the **Table 4.2 & Table 4.3**.

Table 4 2: Rescaling factor

| Rescaling factor | Band 10 | Band 11 |
|------------------|----------|----------|
| M_L | 0.000342 | 0.000342 |
| A_L | 0.1 | 0.1 |

Table 4 3: K1 and K2 values

| Thermal constants | Band 10 | Band 11 |
|-------------------|---------|---------|
| K1 | 1321.08 | 1201.14 |
| K2 | 777.89 | 480.89 |

The steps involved in the retrieval of LST from the algorithm used is shown in the flowchart below.

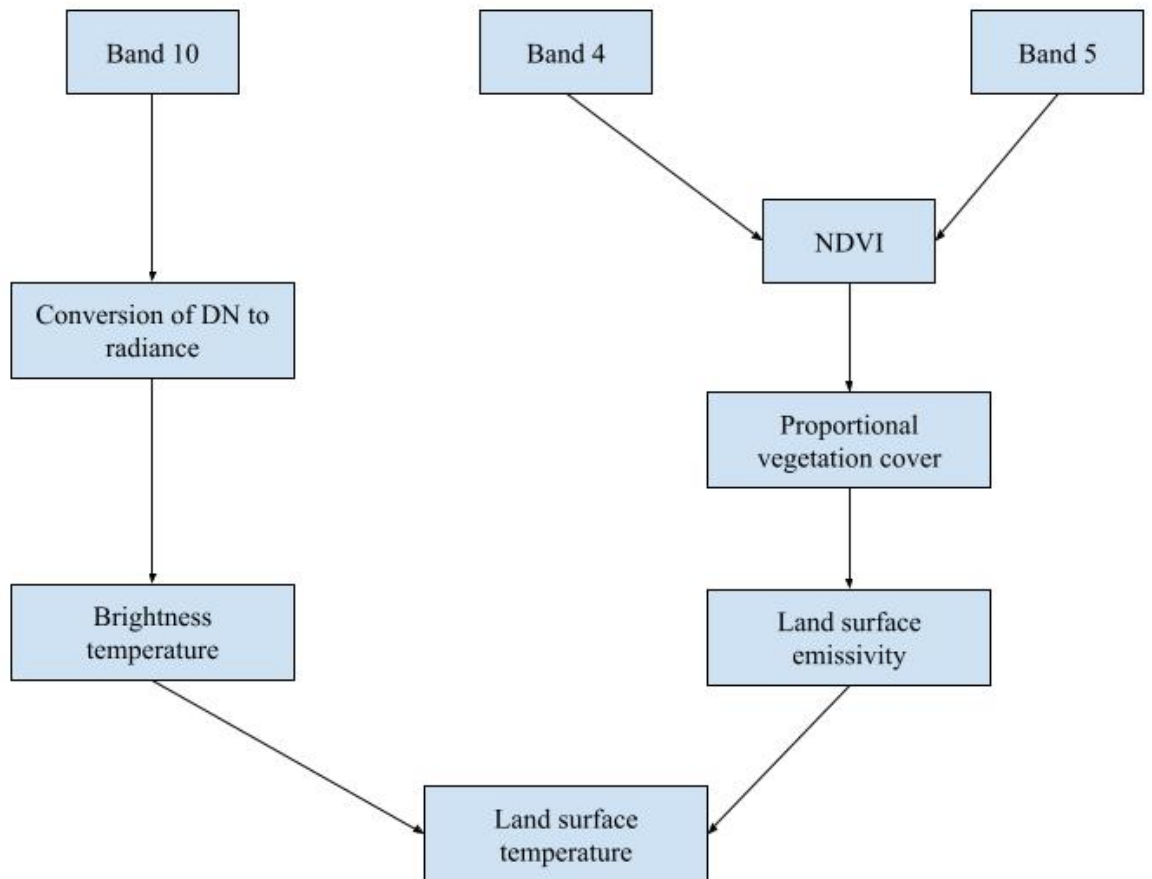


Figure 4. 5: Flowchart of retrieving LST from Landsat 8 image

4.6.1: Conversion of DN to radiance

The first step in LST estimation is the input of band 10. After inputting Band 10 the tool uses formulas taken from the USGS web page for retrieving the top of atmospheric (TOA) spectral radiance ($L\lambda$) from DN values:

$$L\lambda = M_L * Q_{CAL} + A_L \quad (4.1)$$

Where M_L represents the Band specific multiplicative rescaling factor, Q_{CAL} is the band 10 image, and A_L is the band specific additive rescaling factor.

4.6.2: Brightness temperature

After converting the DN values to at-sensor spectral radiance, the TIRS band data should be converted to brightness temperature (BT) using the thermal constant given in the metadata file and the following equation:

$$BT = \frac{K_1}{\ln\left[\left(\frac{K_2}{L\lambda}\right)+1\right]} \quad (4.2)$$

Where, K_1 and K_2 are the thermal constants of TIR band 10

$$K_1 = 774.8853$$

$$K_2 = 1321.0789$$

4.6.3: Normalized difference vegetation index (NDVI)

The NDVI represents the dimensionless index which reflects here the variation in plant reflectance among visible and near-infrared light which may be used to assess the density of green areas in the area of interest. The NDVI varies in ranges from -1 to +1. Higher NDVI values which represent indicate healthy and thick vegetation, whereas lower NDVI values indicate sparse vegetation. The NDVI is calculated by dividing the total of near-infrared (NIR) and red (RED) reflectance by their difference. Band 5 is the NIR band for Landsat 8 data, whereas Band 4 is the Red Band.

$$NDVI = \frac{(NIR - RED)}{(NIR + RED)} \quad (4.3)$$

4.6.4: Normalized difference Built-up index (NDBI)

This index here observes urban areas with higher reflectance with in shortwave-infrared (SWIR) area of interest apart from the near-infrared (NIR) region. Watershed runoff projections and land-use blue print organizing are two examples of applications. The NDBI was first designed to work by having the data from Landsat TM bands 5 and 4.

Here, however, function for the used multispectral sensor having the SWIR band of 1.55-1.75 m and an NIR band of 0.76-0.9 m.

$$NDBI = \frac{(SWIR - NIR)}{(SWIR + NIR)} \quad (4.4)$$

The Normalized Difference Built-up Index value is present in middle of -1 to +1. Negative values of NDBI shows the water sources whereas higher values signify build-up region. The NDBI value for the area of interest vegetation is comes out low.

4.6.5: Proportional vegetation cover

The comparable vegetation calculates the area affected by each land cover category. The proportions of greenery and bare soil are calculated using the NDVI for pure pixels. In global settings, values of $NDVIV = 0.5$ and $NDVIS = 0.2$ have been suggested. Equation may be used to compute PV. (4.5)

$$P_V = \left(\frac{(NDVI - NDVIS)}{(NDVIV - NDVIS)} \right)^2 \quad (4.5)$$

4.6.6: Land surface emissivity

Surface emissivity is the ability of a surface to convert heat energy into radiant energy. LSE () is a critical metric for obtaining correct LST via remotely sensed imagery. The following equation is used to compute LSE:

$$\epsilon_\lambda = \epsilon_{V\lambda} P_V + \epsilon_{S\lambda} (1 - P_V) + C_\lambda \quad (4.6)$$

Were,

$\epsilon_{V\lambda}$ and $\epsilon_{S\lambda}$ are the vegetation and soil emissivity respectively and c_λ is the surface roughness

Taken as a constant value of 0.005.

The mean emissivity of significant land cover types can be regarded in band 10 as follows: once the NDVI becomes less than 0, it is labelled as water and an emissivity value of 0.991 is assigned; when the NDVI is between 0 and 0.2, it is classified as soil and an emissivity value of 0.996 is assigned; and when the NDVI is greater than 0.5, it is classified as vegetation and an emissivity value of 0.973 is assigned.

4.6.7: Land surface temperature

The calculation of LST comes at the last computing brightness temperature (BT) of band 10 and Land surface emissivity value that are obtained from Pv and NDVI. The Land surface temperature T_s is observed by using the below formula:

$$T_S = \left(\frac{BT}{\left[1 + \left\{ \left(\frac{\lambda BT}{\rho} \right) \ln \epsilon_\lambda \right\} \right]} \right) - 273.15 \quad (4.7)$$

Where,

T_s represents temperature in Celsius ($^{\circ}c$)

BT represents at-sensor brightness temperature ($^{\circ}c$)

λ is the mean wavelength of band 10 (10.895 μ m)

ρ is ($h \cdot c / \sigma$) (1.438 $\cdot 10^{-2}$ mK) here, σ denotes Boltzmann constant (1.38 $\cdot 10^{-23}$ j/k), h denotes Plank constant (6.626 $\cdot 10^{-34}$ js) and c represents here the speed of light that is (3 $\cdot 10^8$ m/s).

ϵ_λ is the emissivity equation (4.6)

Results obtained from the Calculation of Land surface temperature are tabulated in **Table 5.2** and the LST maps of the different years are shown in the figures below.

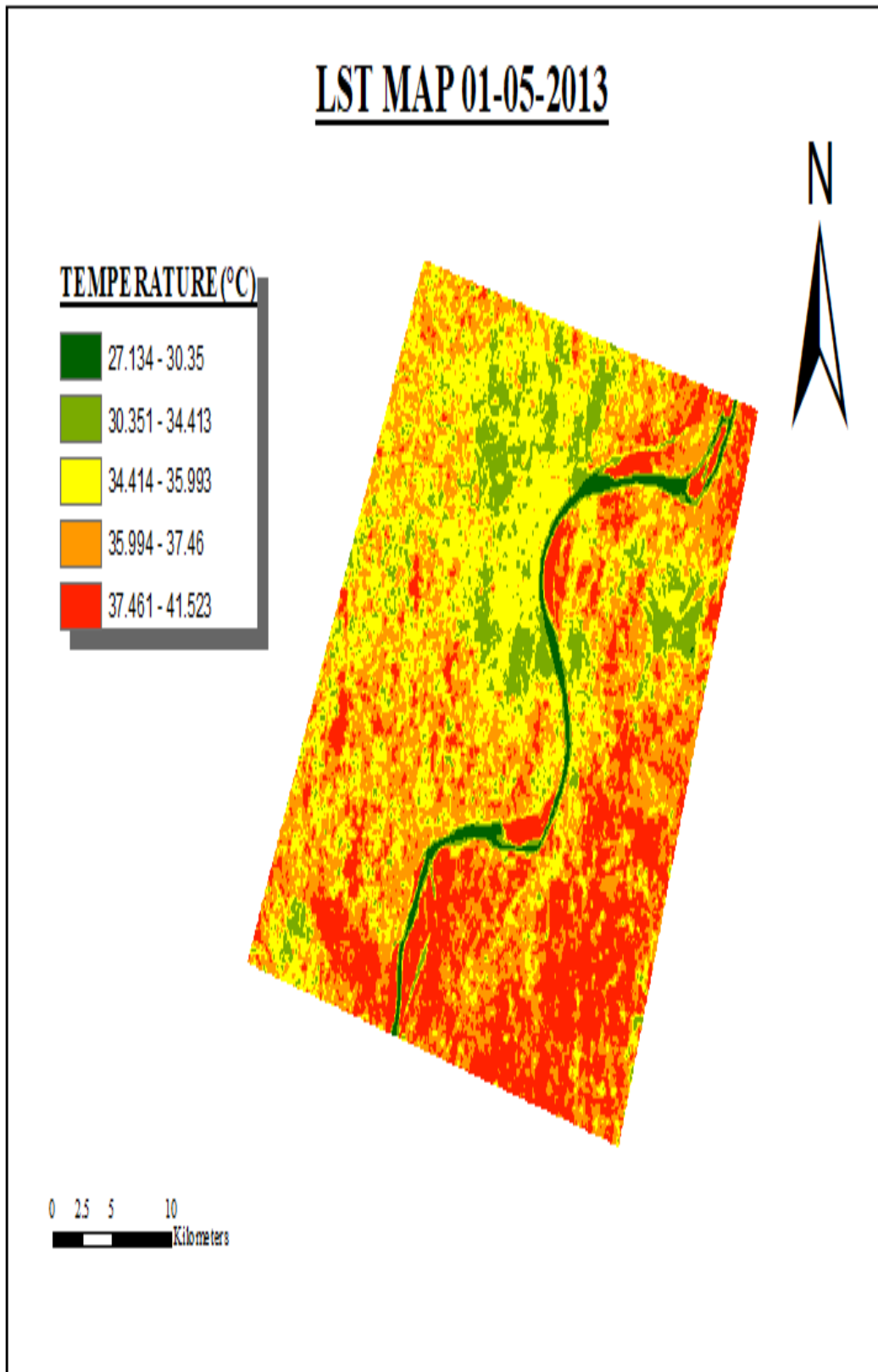


Figure 4. 6: LST map of study area 01-05-2013

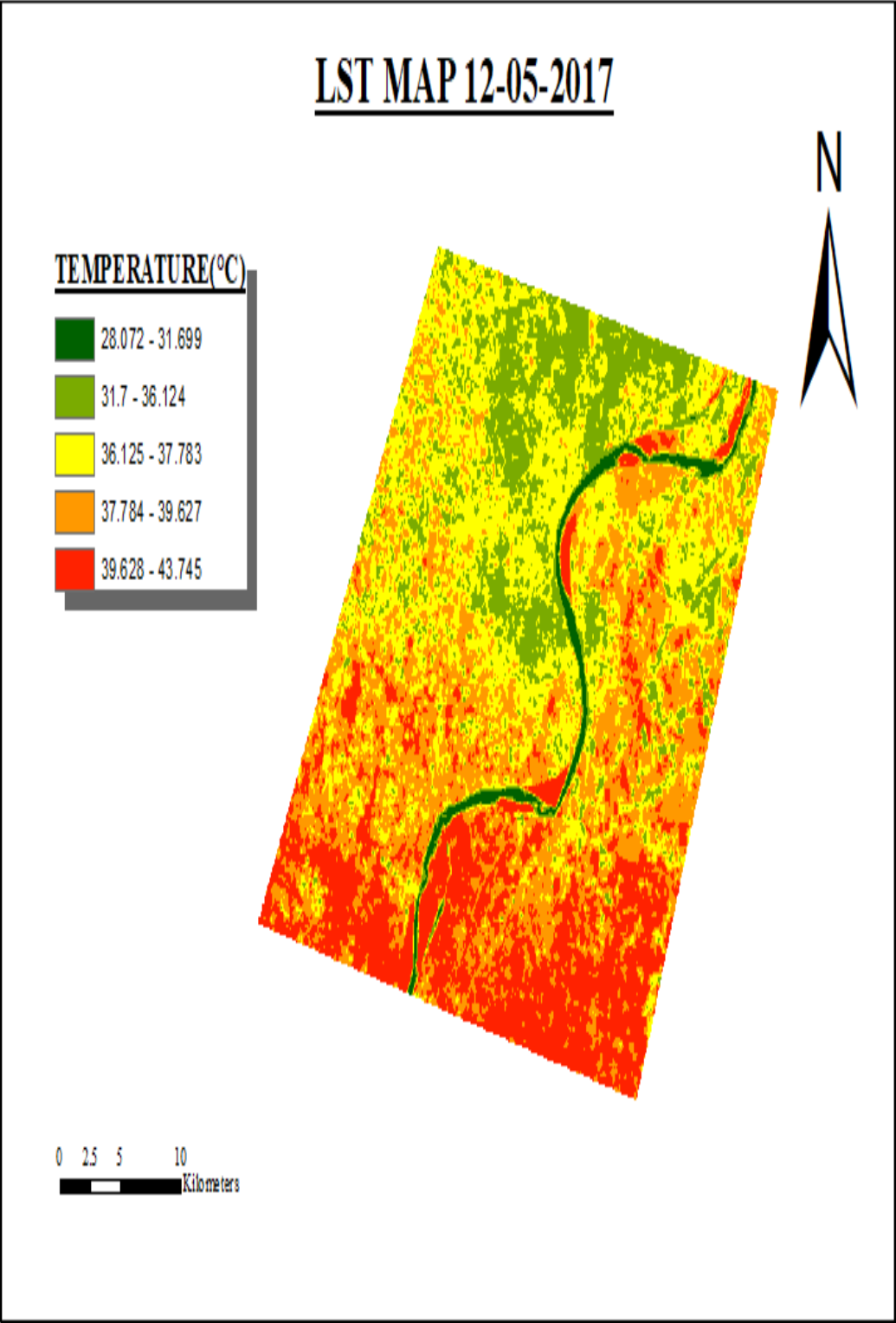


Figure 4. 7: LST map of study area 12-05-2017.

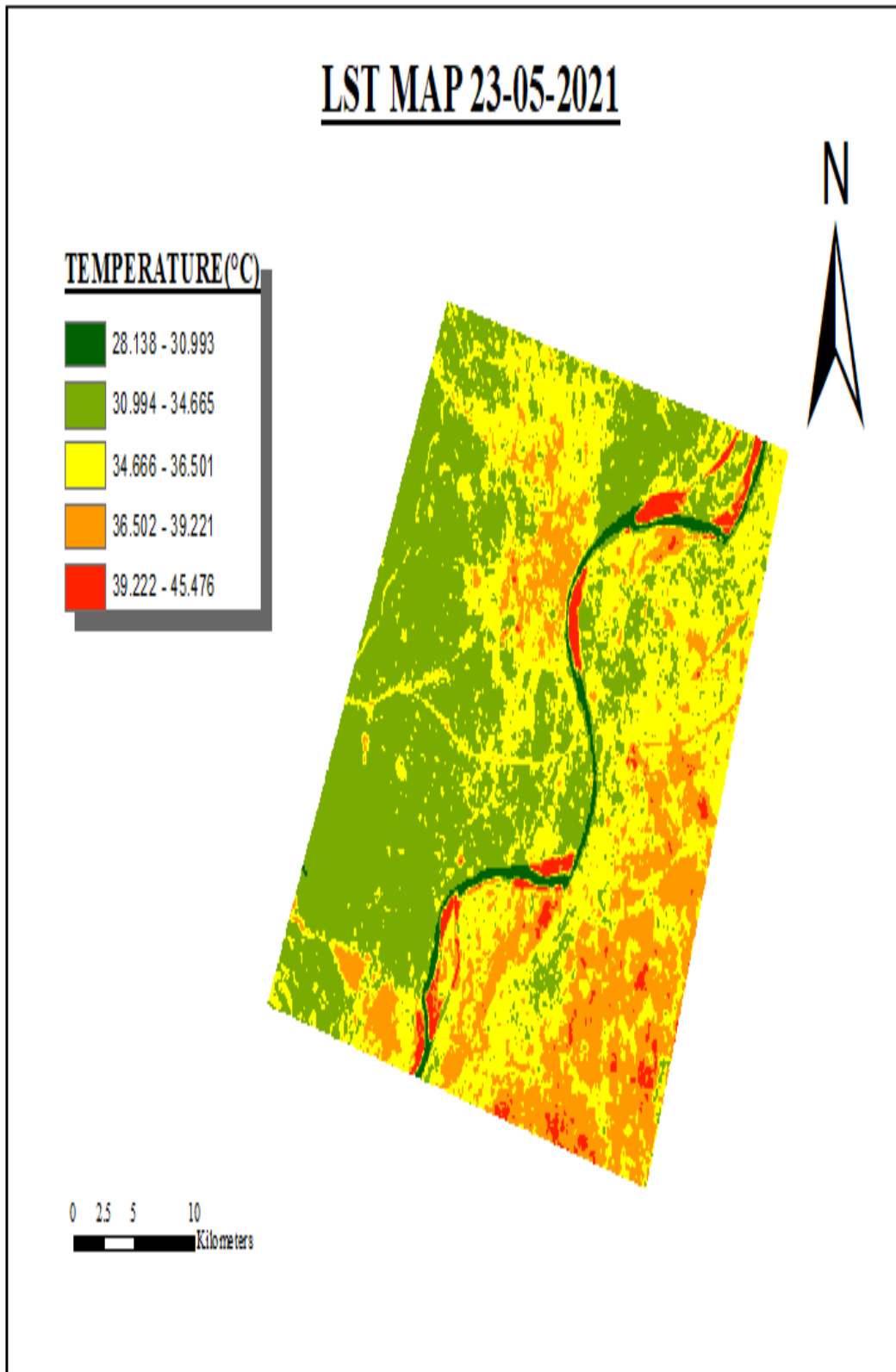


Figure 4. 8: LST map of study area 23-05-2021

4.7: LST Variation with Different LULC Classes

Following the compilation of LST by getting the Landsat 8 satellite dataset, the LST data was utilized for observing the effect of various Land use/Land cover classifications on LST. This analysis attempted to investigate the geographical and temporal fluctuation LST for different LULC classes. This research was carried out using the ARCGIS 10.8 program Table 5.3 shows the results of this investigation, and the figures below indicate the change of land surface temperature for different LULC classes have been shown in the figures below:

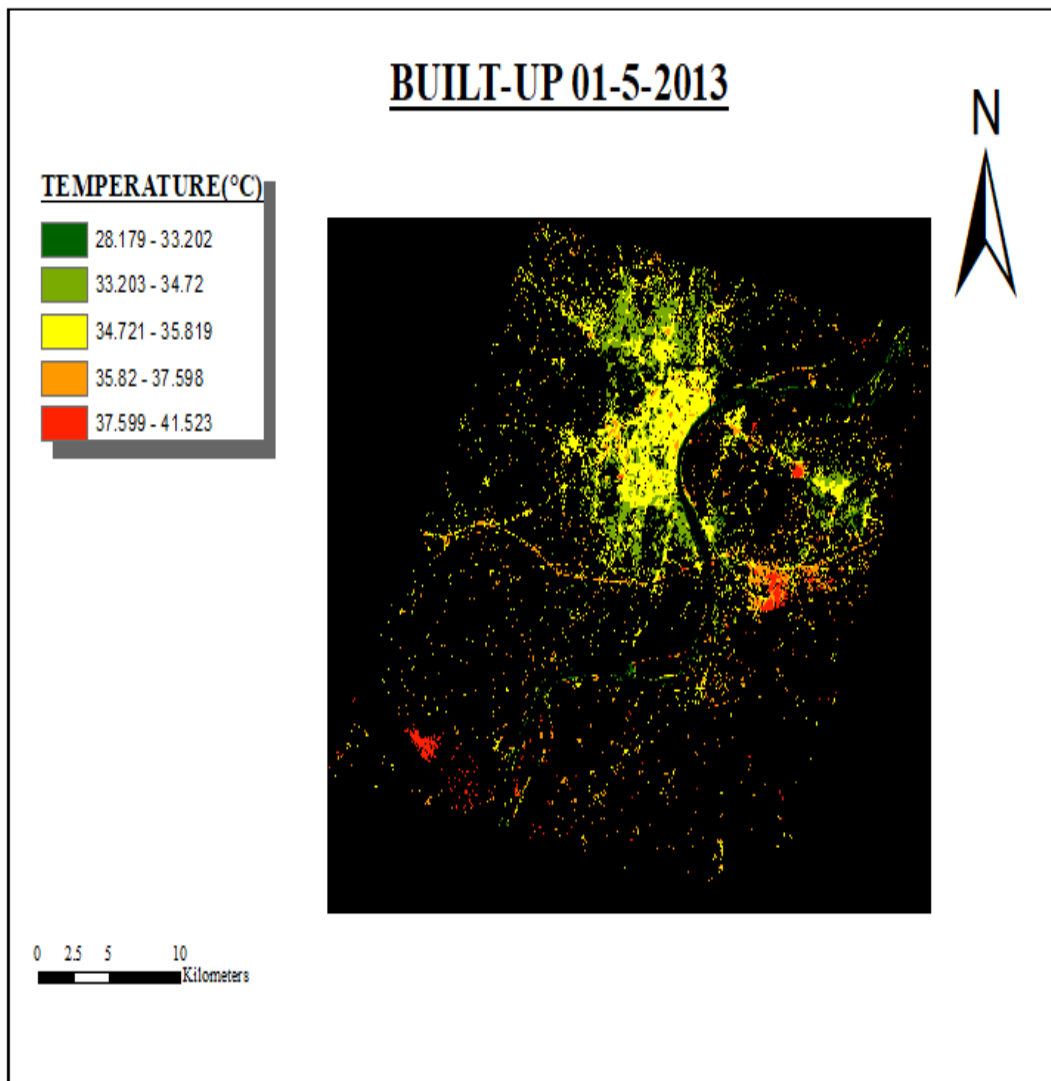


Figure 4. 9: Variation of LST with Built-up 01-05-2013

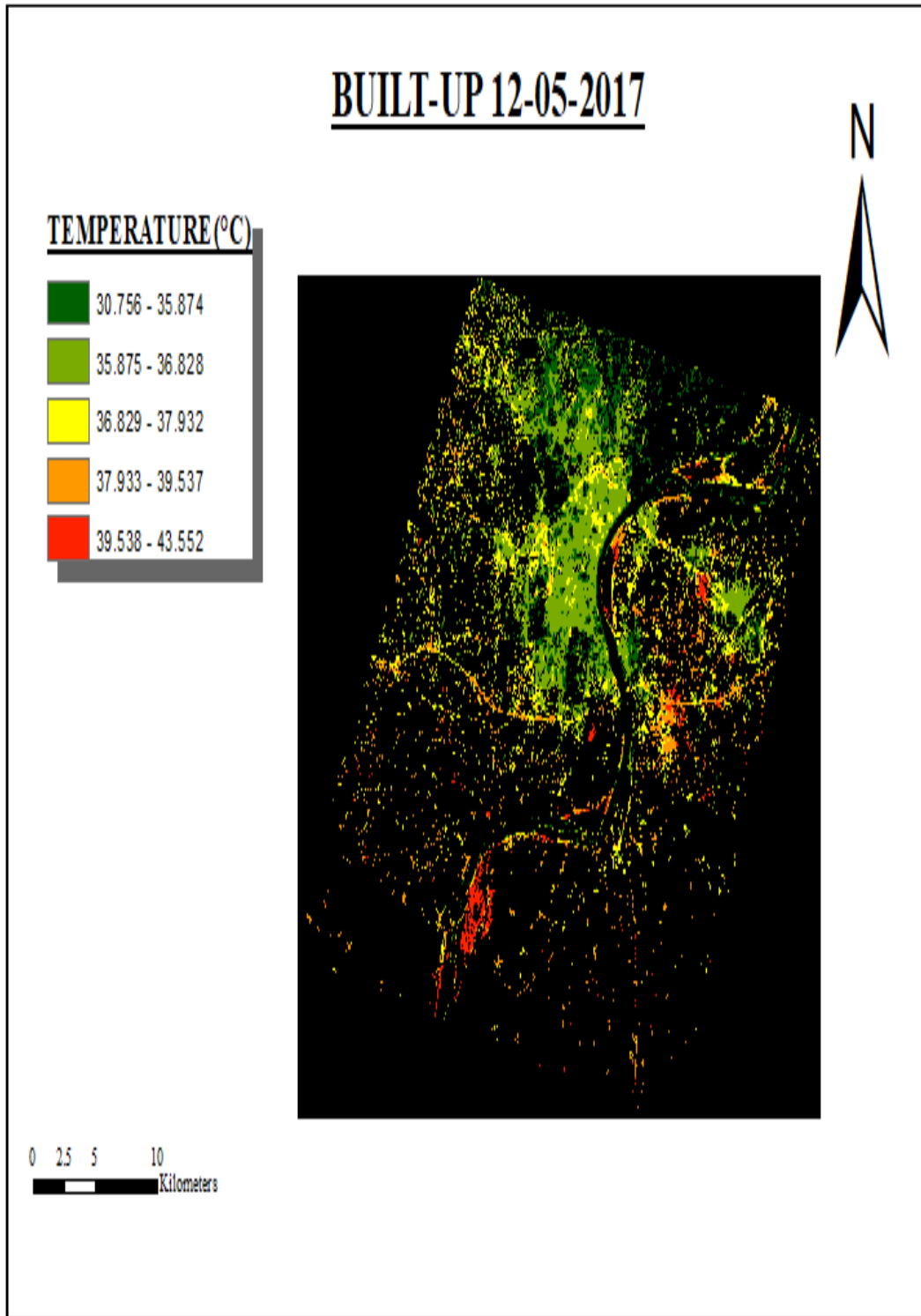


Figure 4. 10: Variation of LST with Built-up 12-05-2017

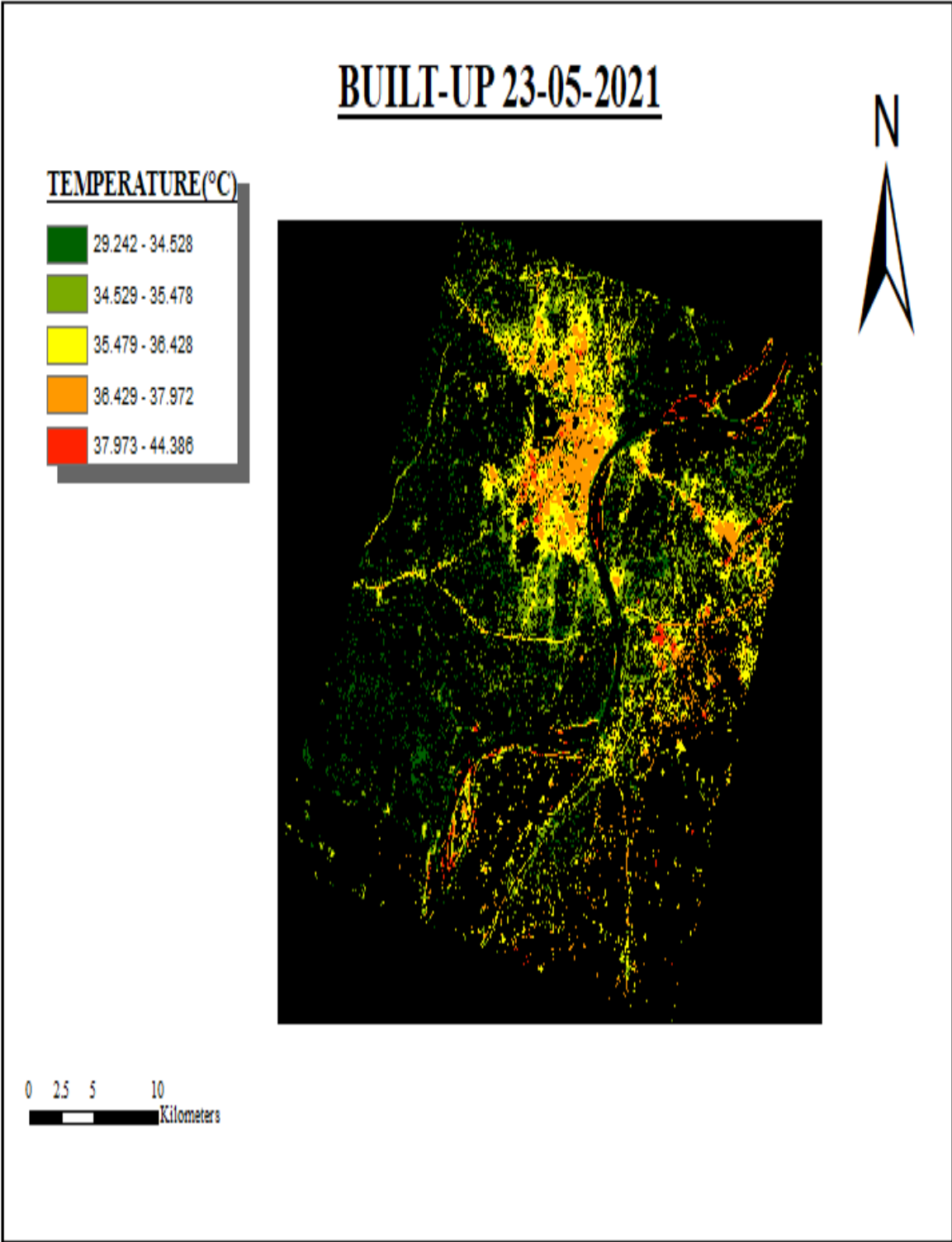


Figure 4. 11: Variation of LST with Built-up 23-05-2021

FALLOW LAND 01-05-2013

TEMPERATURE (°C)

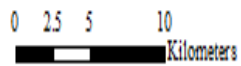
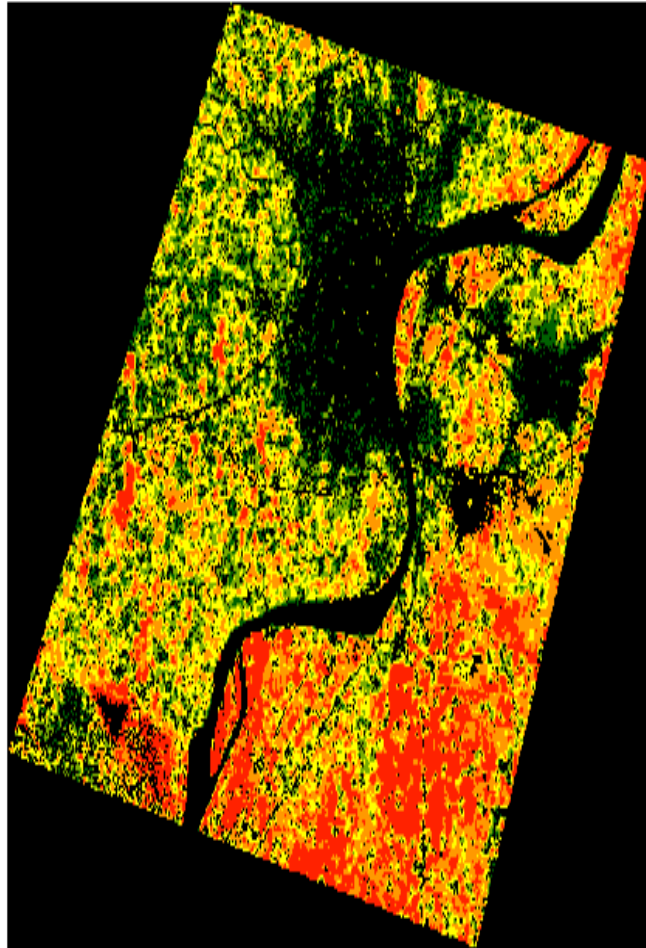
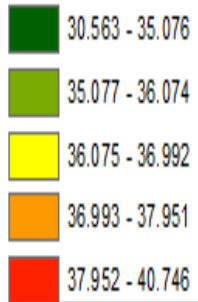


Figure 4. 12: Variation of LST with Fallow land 01-05-2013

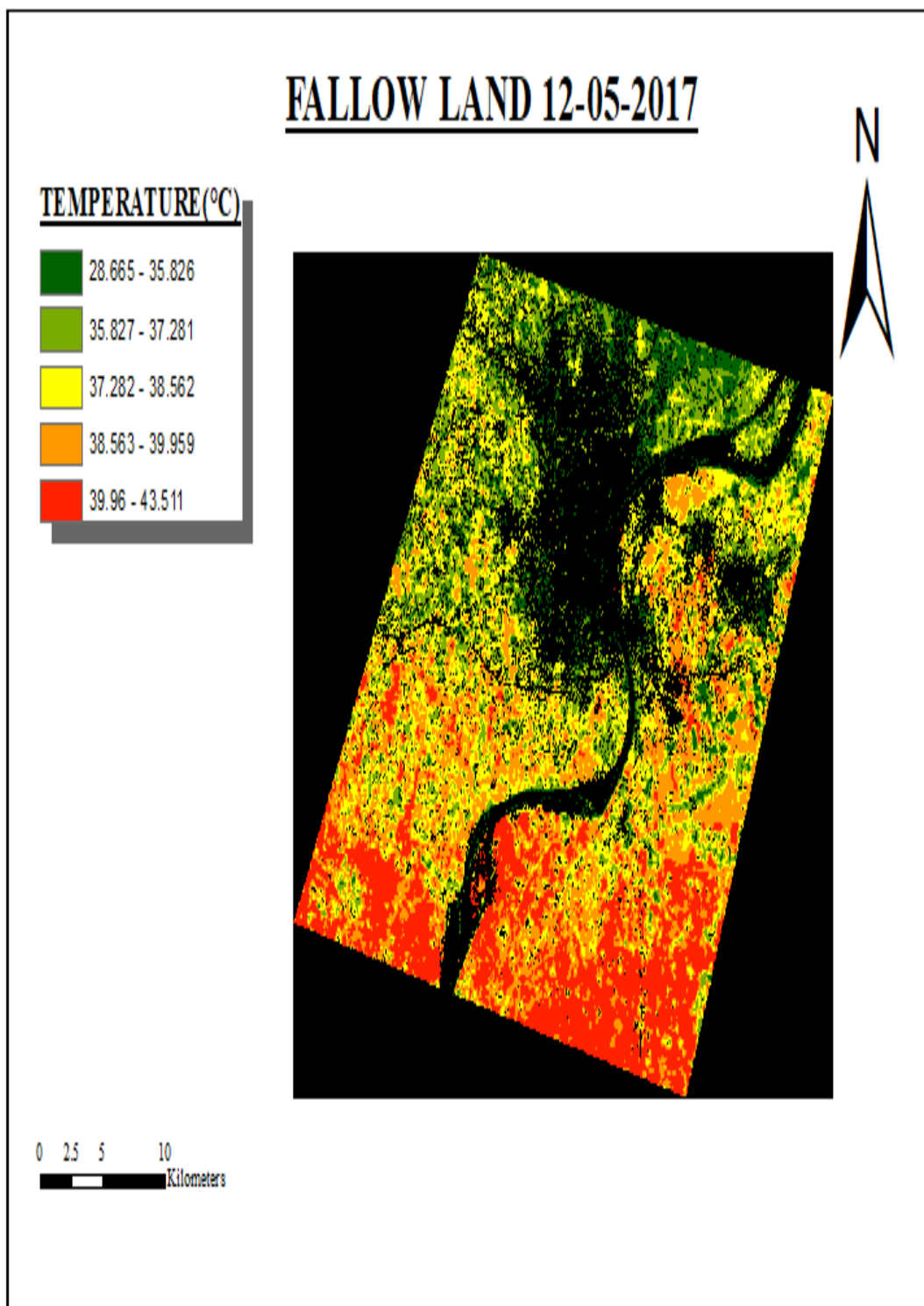


Figure 4. 13: Variation of LST with Fallow land 12-05-2017

FALLOW LAND 23-05-2021

TEMPERATURE (°C)

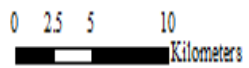
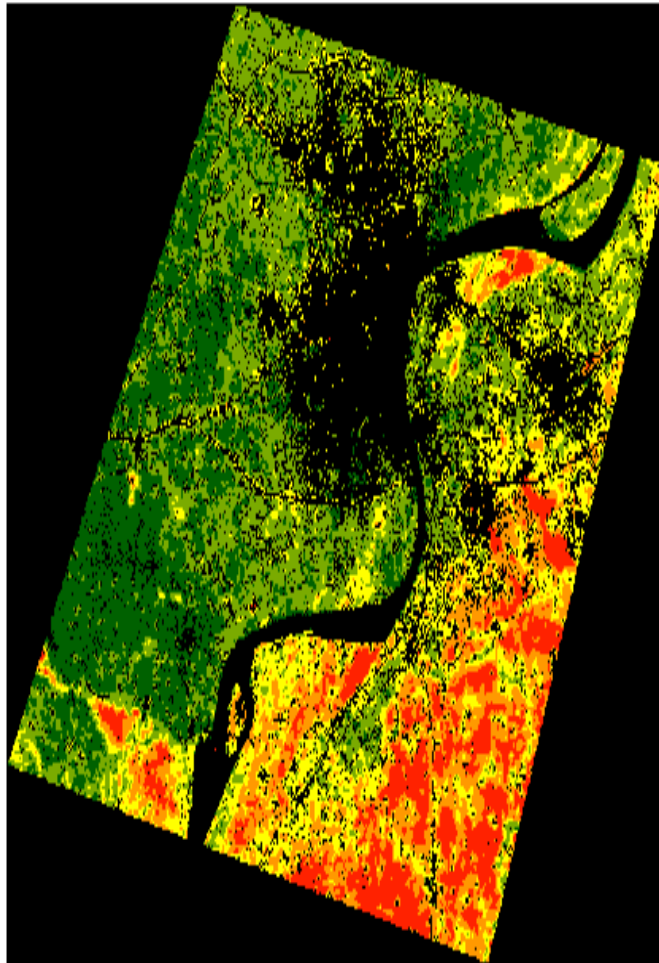
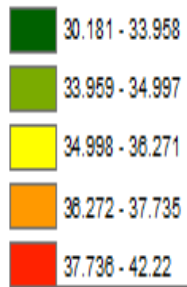


Figure 4. 14: Variation of LST with Fallow land 23-05-2021

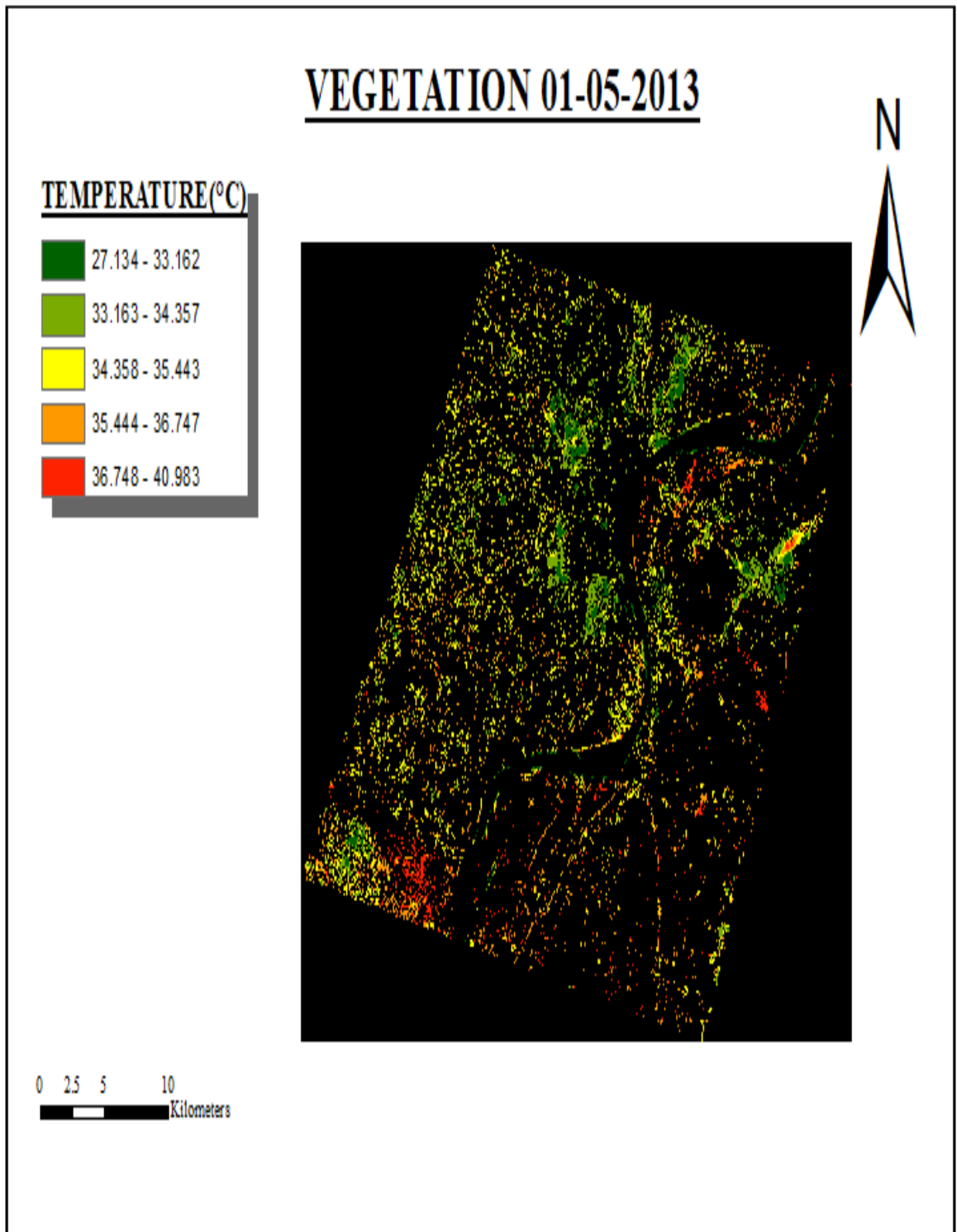


Figure 4. 15: Variation of LST with Vegetation 01-05-2013

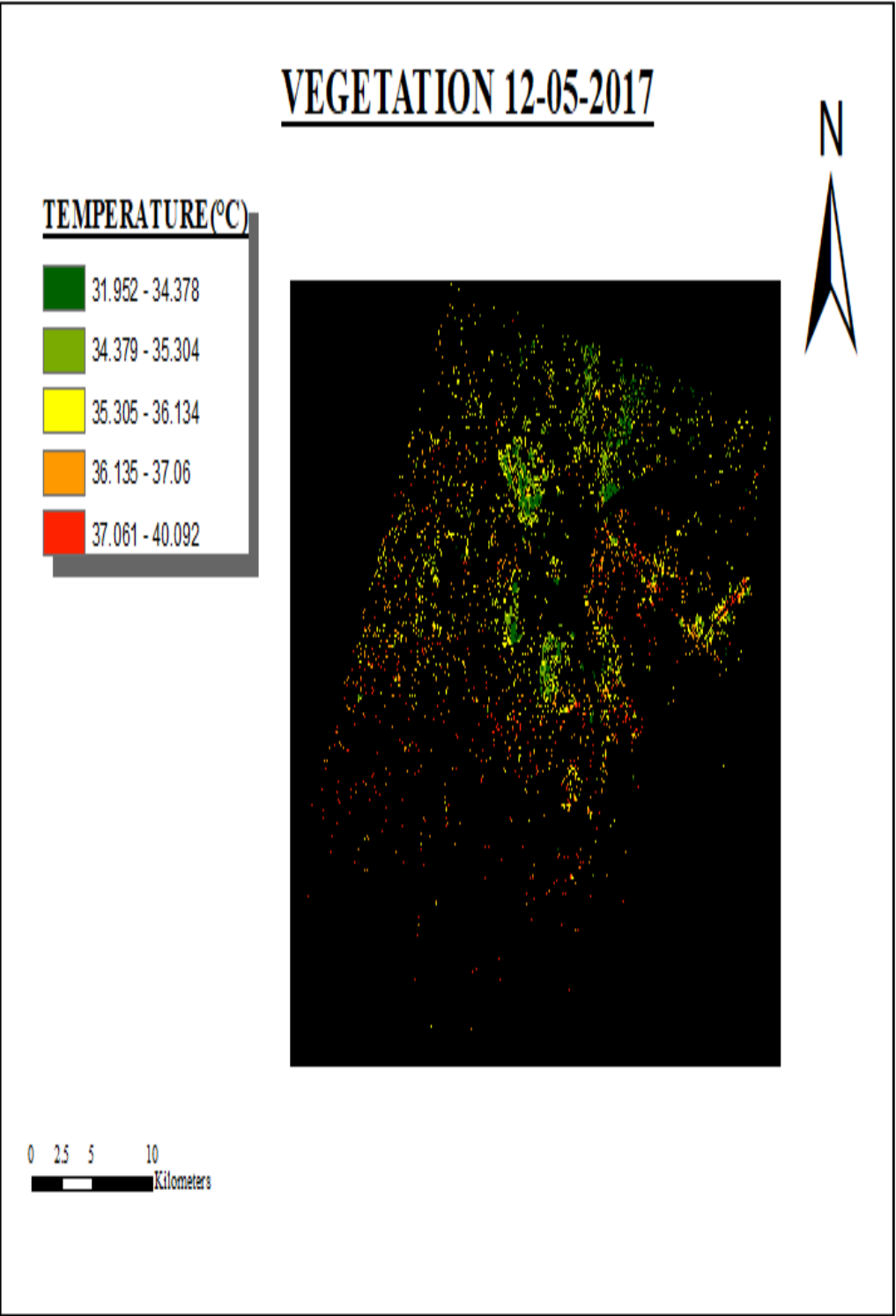


Figure 4. 16: Variation of LST with Vegetation 12-05-2017

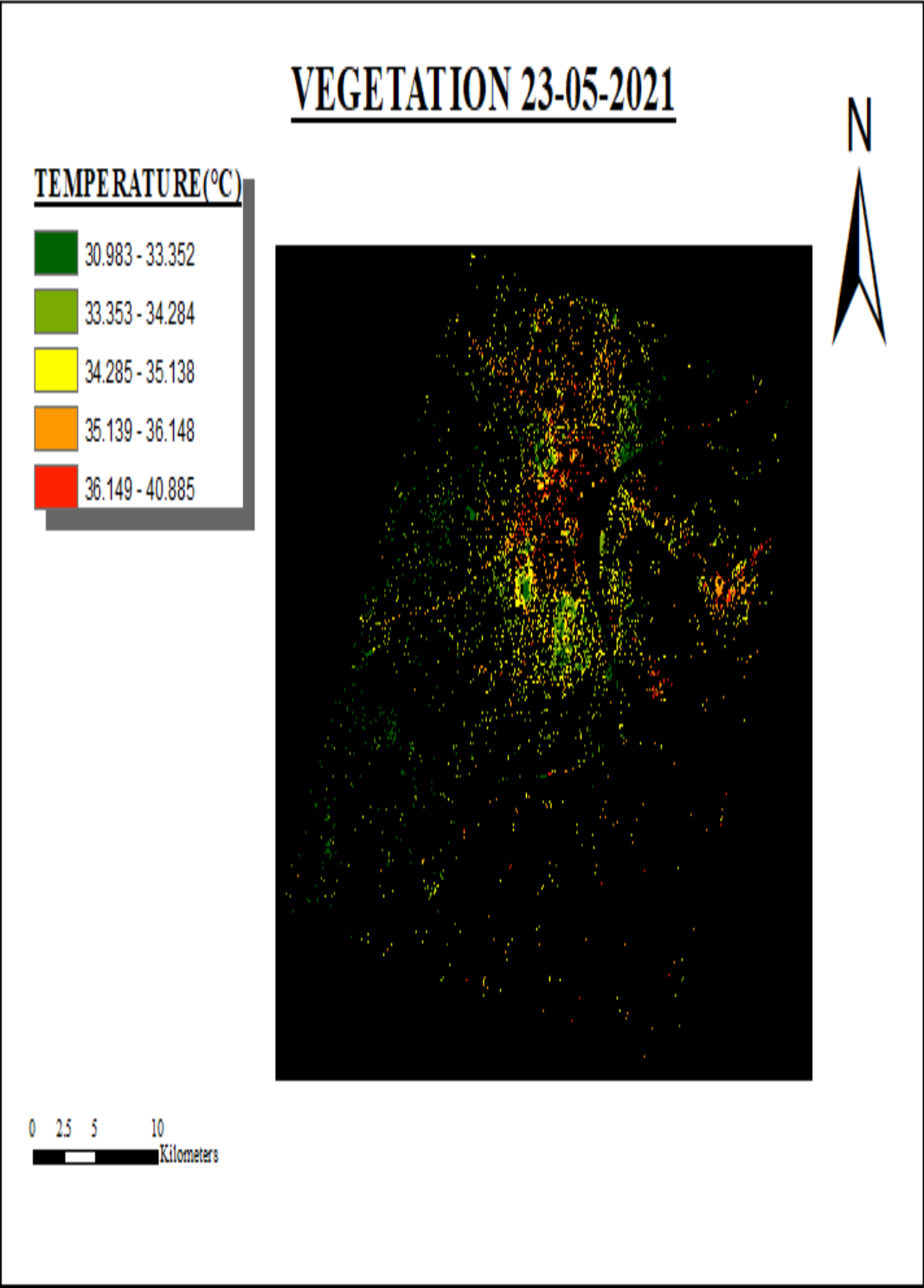


Figure 4. 17: Variation of LST with Vegetation 23-05-2021

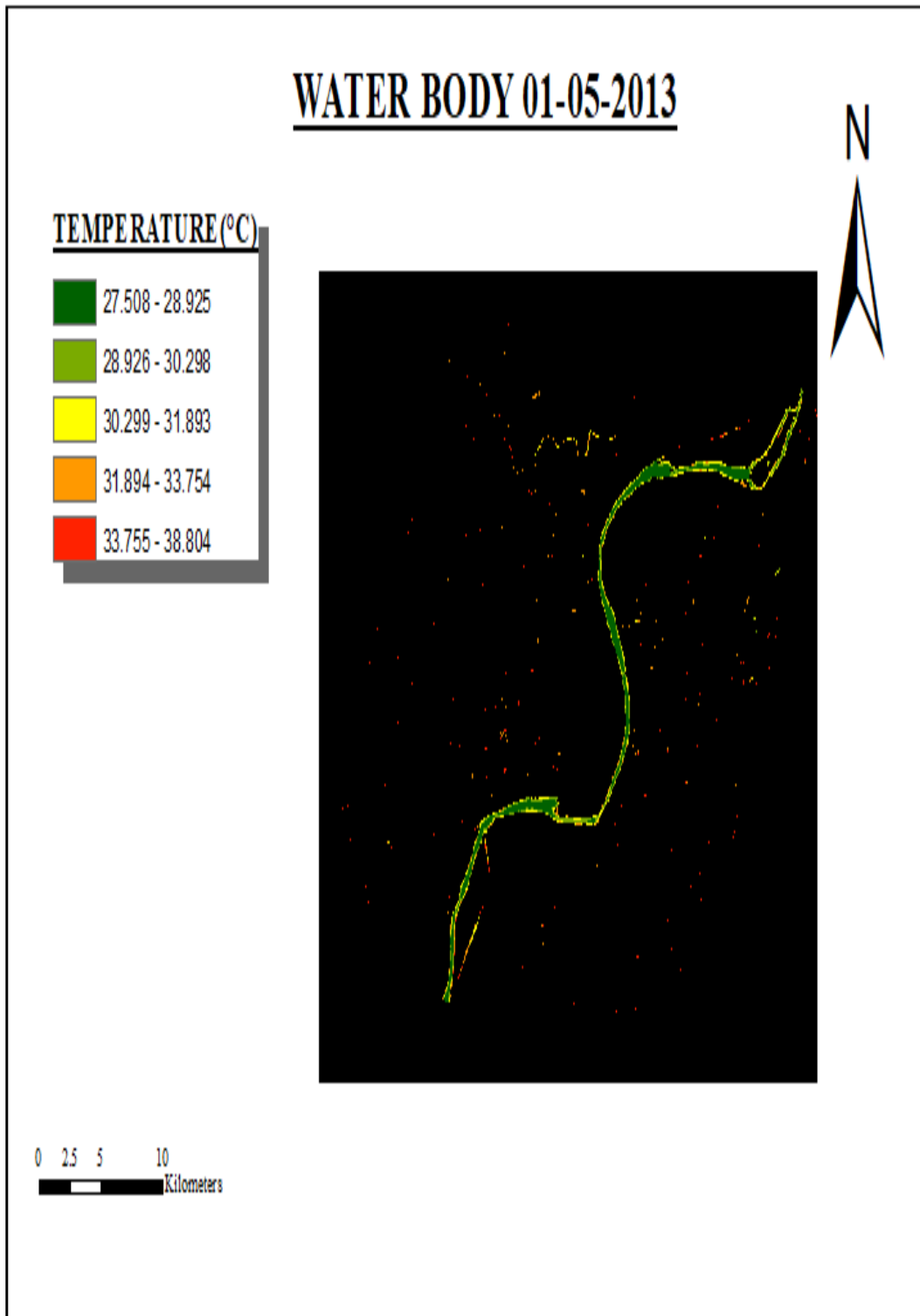


Figure 4. 18: Variation of LST with Waterbody 01-05-2013

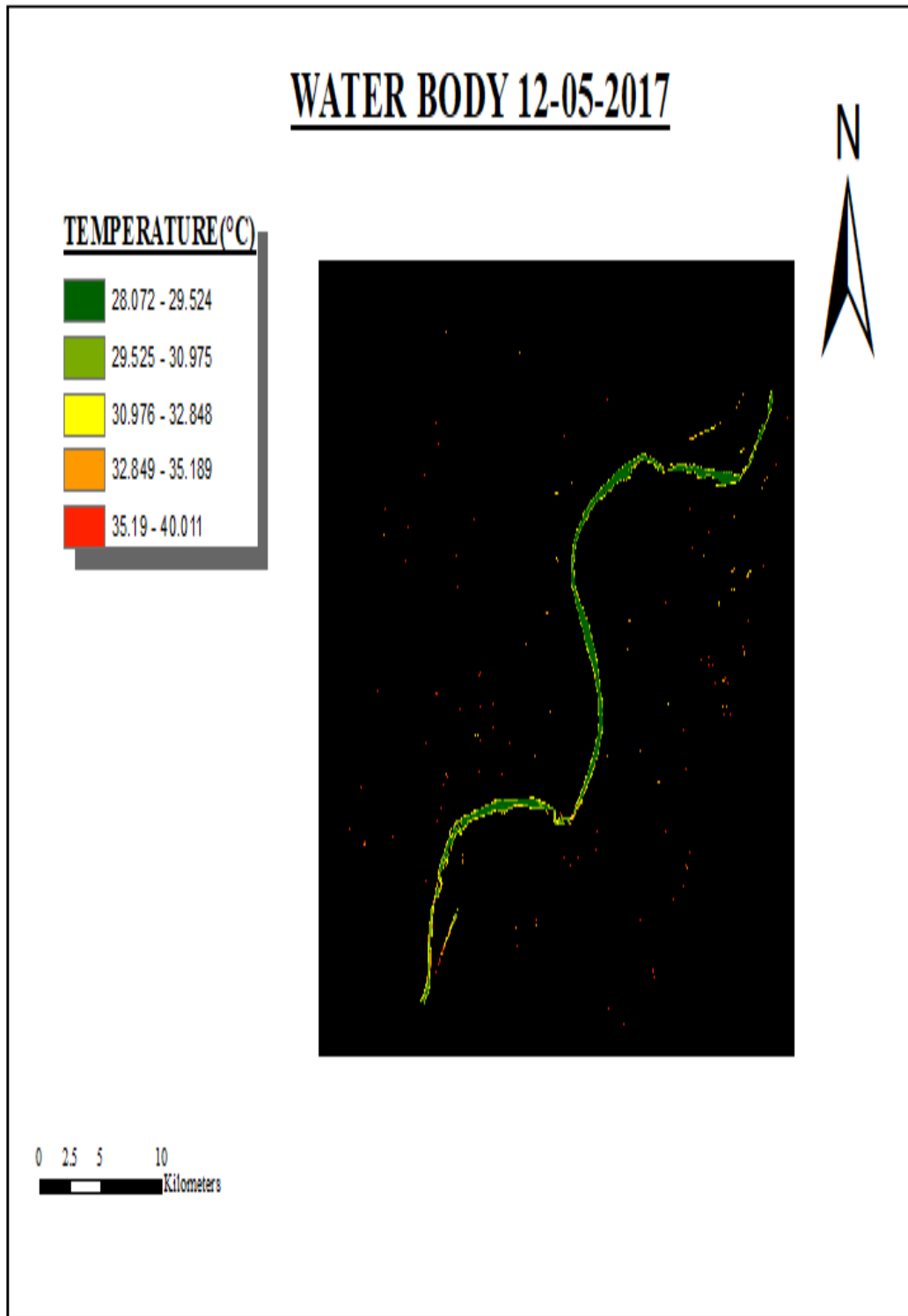


Figure 4. 19: Variation of LST with Waterbody 12-05-2017

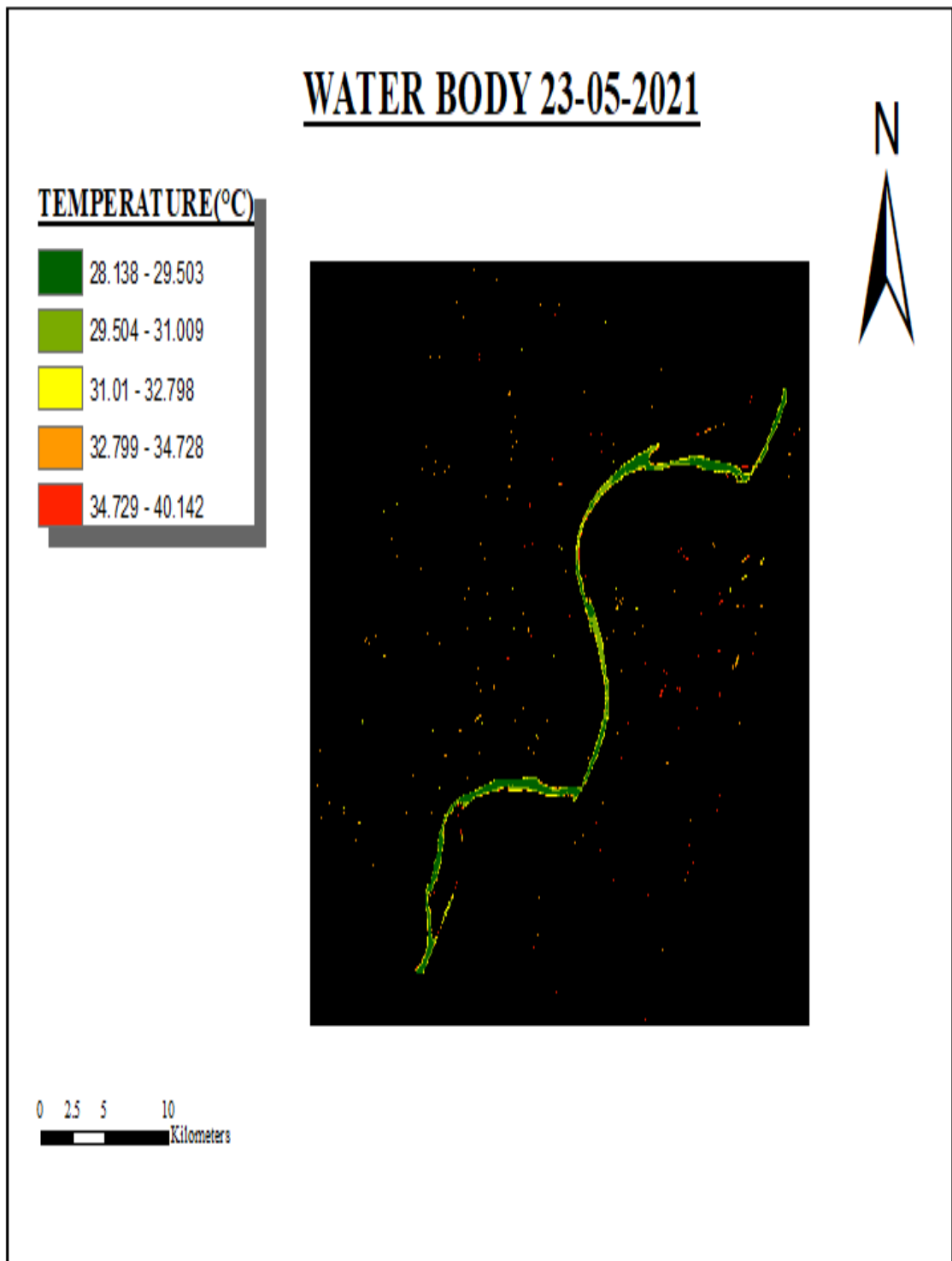


Figure 4. 20: Variation of LST with Waterbody 23-05-2021

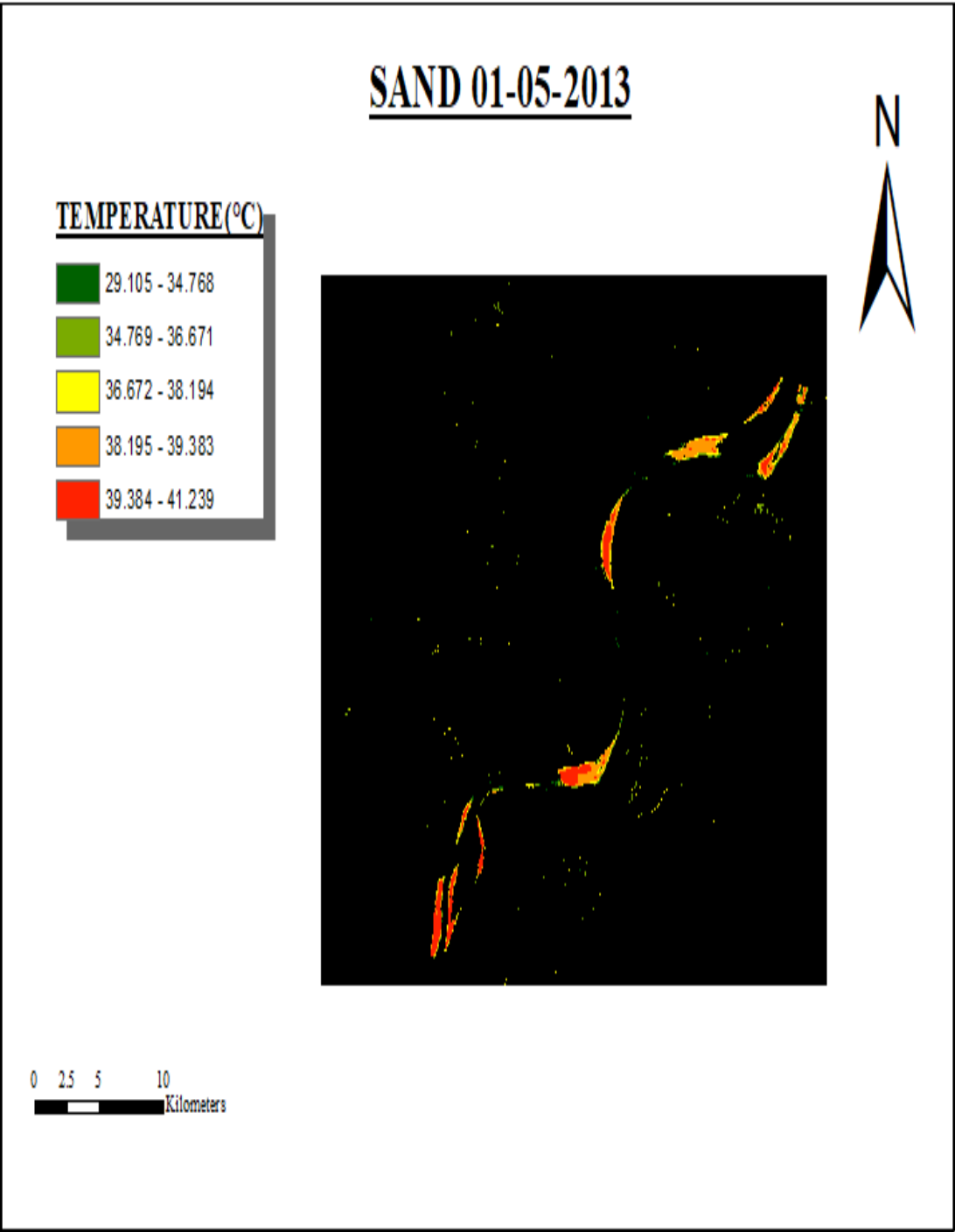


Figure 4. 21: Variation of LST with Sand 01-05-2013

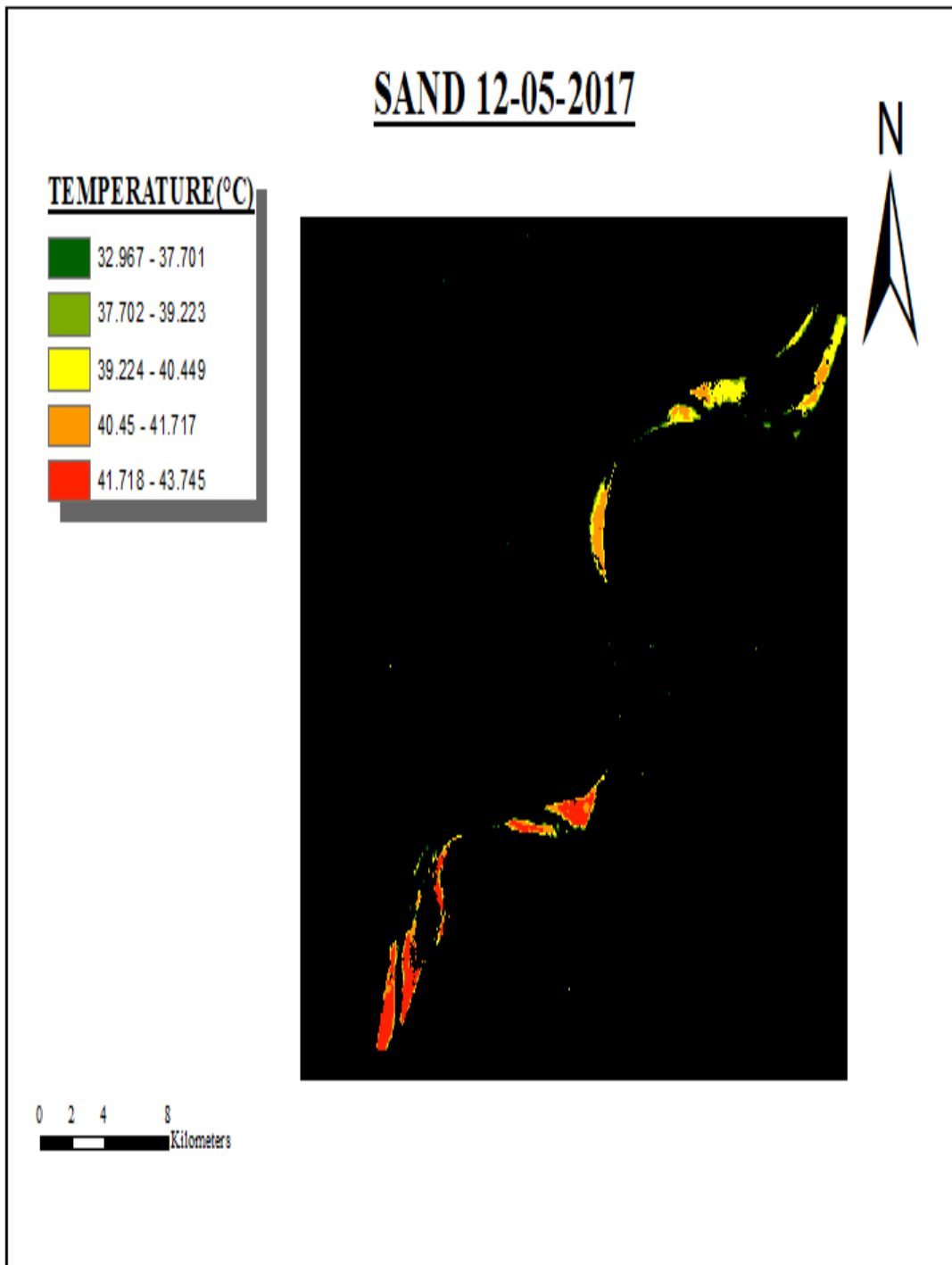


Figure 4. 22: Variation of LST with Sand 12-05-2017

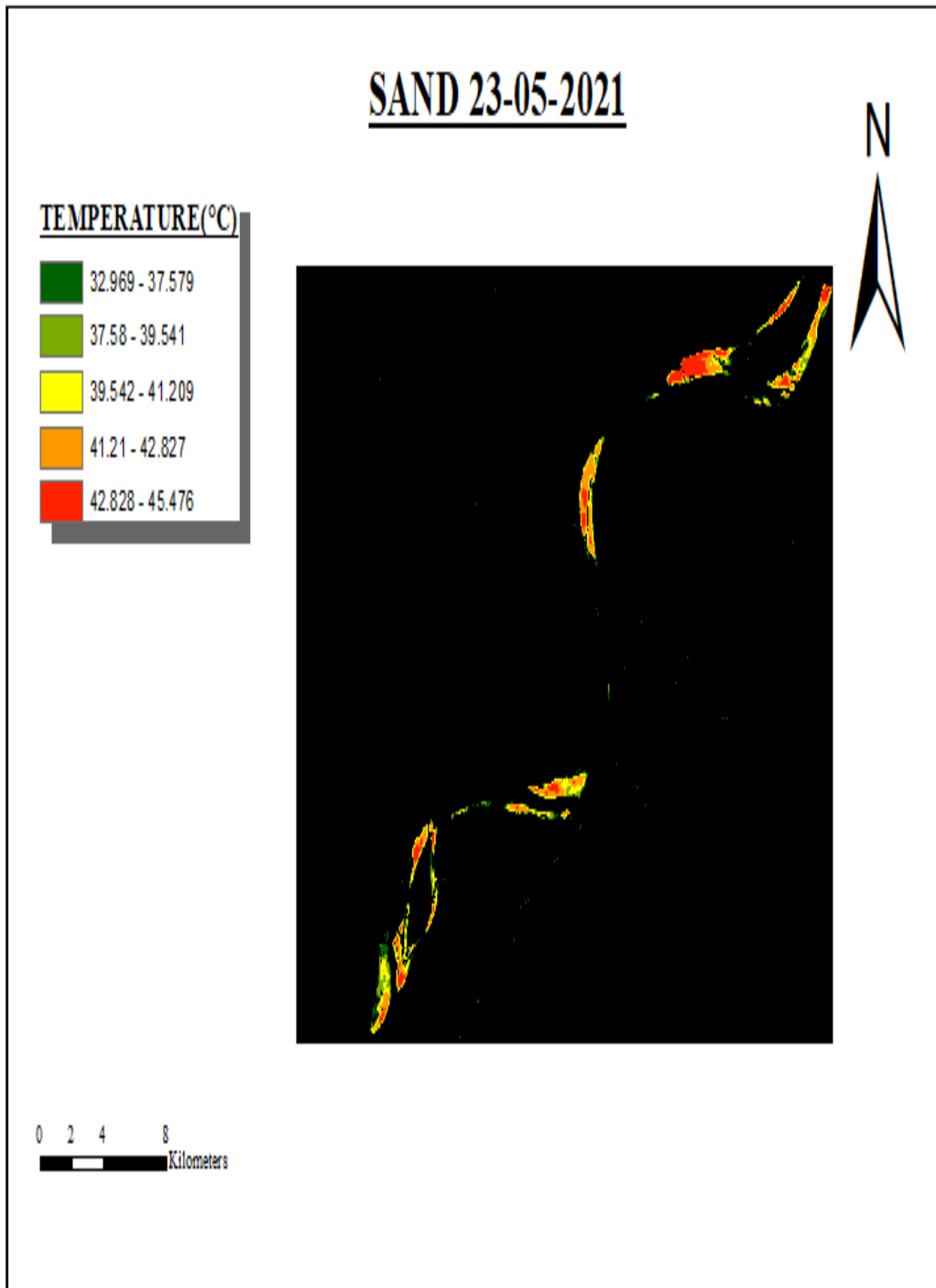


Figure 4. 23: Variation of LST with Sand 23-05-2021

4.8: Correlation Analysis

Correlation analysis was performed using ARCGIS 10.8 software, in which the pattern similarity of LST with the NDVI and NDBI was analyzed in this analysis multiple number of points were selected by creating a fishnet on the raster dataset of LST, NDVI and NDBI. After that, the attribute table of these data sets were used to create a scatter graph of LST with NDVI and LST with NDBI. The scatter plot showing trend analysis of correlation are given in the figure below:

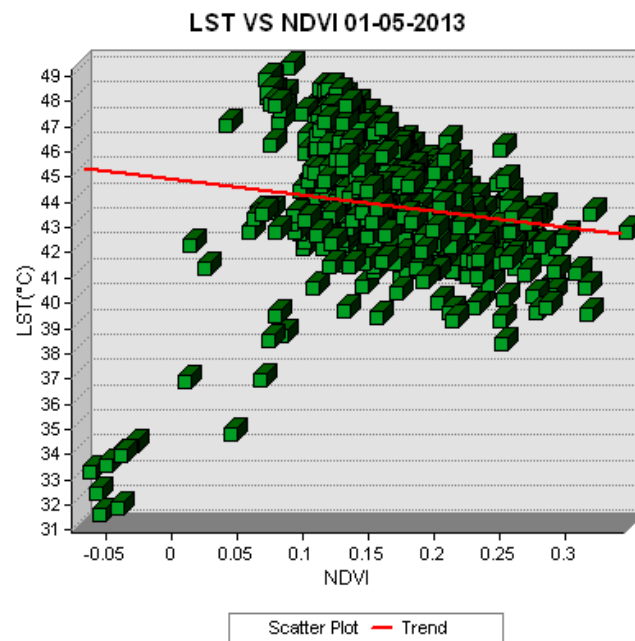


Figure 4. 24: Trend analysis of LST with NDVI 01-05-2013

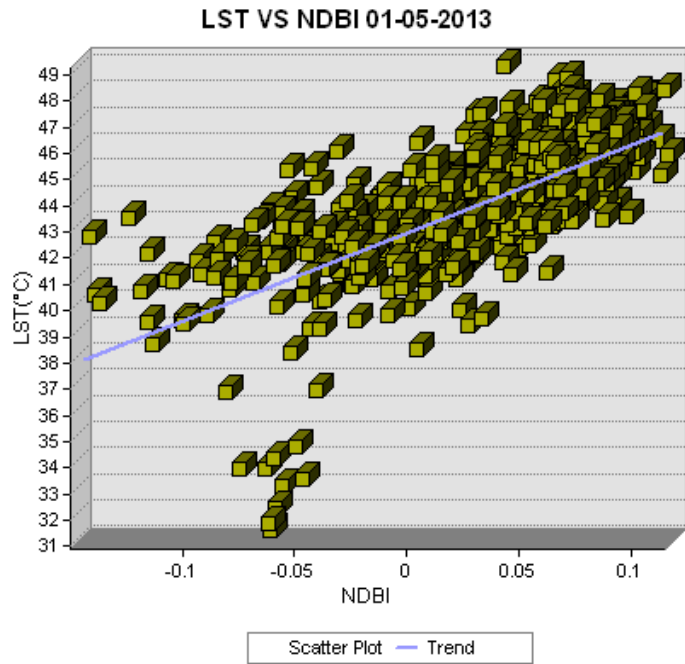


Figure 4. 25: Trend analysis of LST with NDBI 01-05-2013

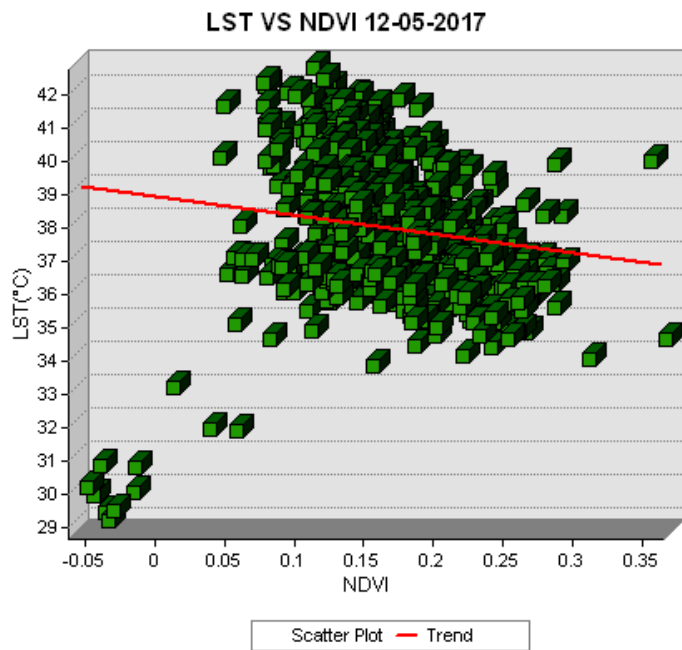


Figure 4. 26: Trend analysis of LST with NDVI 12-05-2017

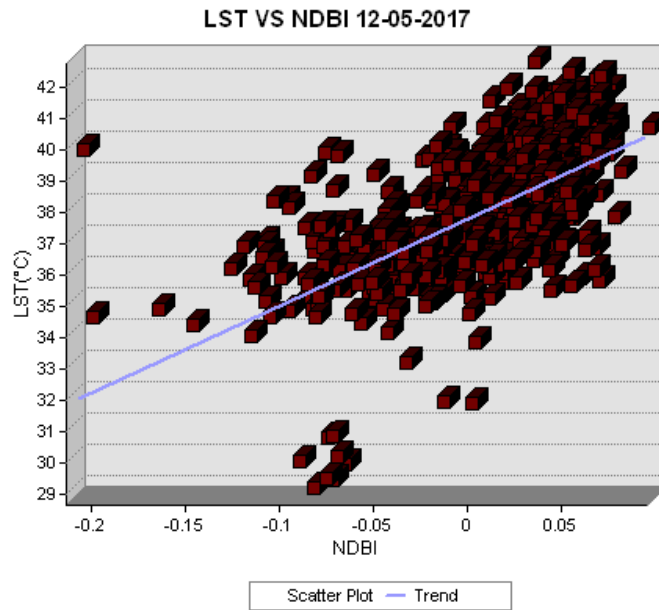


Figure 4. 27: Trend analysis of LST with NDBI 12-05-2017

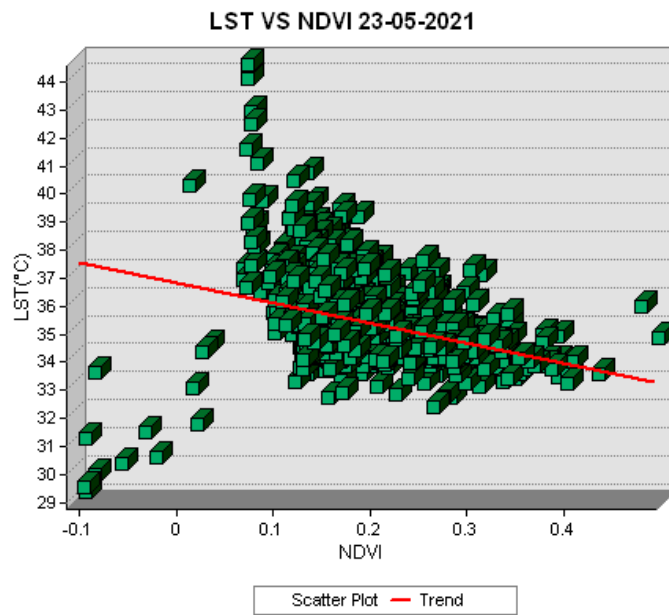


Figure 4. 28: Trend analysis of LST with NDVI 23-05-2021

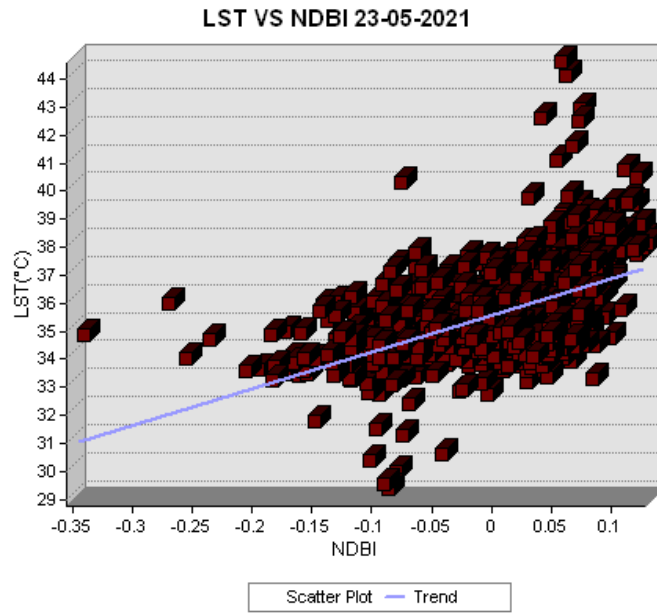


Figure 4. 29: Trend analysis of LST with NDBI 23-05-2021

CHAPTER 5

RESULTS & DISCUSSION

The LULC maps for 2013, 2017 and 2021 were prepared by classifying the Landsat 8 images using maximum likelihood classifier in Erdas Imagine 2015 software. The LULC changes were analyzed using the LULC map the result of which is shown in the **Table 5.1**.

Table 5. 1: LULC classes and their areas in different years

| LULC classes | Area may 2013 (sq. km) | Area may 2017 (sq. km) | Area may 2021 (sq. km) |
|--------------|---------------------------|---------------------------|---------------------------|
| Built-up | 121.7 | 178.65 | 200.38 |
| Waterbody | 22.57 | 19.01 | 22.18 |
| Vegetation | 122.76 | 45.15 | 48.43 |
| Sand | 19.62 | 17.91 | 16.98 |
| Fallow land | 626.83 | 652.75 | 625.52 |

From the **Table 5.1** it can be analyzed that Built-up area has grown from 13.32% (2013) to 19.55% (2017) finally 21.94% (in 2021) of total area (913.48 km²), and subsequently the vegetative land area has decreased significantly from 13.44% (in 2013) to only 4.94 % (in 2017), it shows slight increase from 2017 to 2021 (5.30%) that may be attributed to the urban plantation. With the period of eight years 2013 to 2021 it is seen that the Built-up area has grown with 8.62% of total area (913.48 km²). With maximum growth in Built-up area came out due to change of vegetative land and fallow land to other areas

where concrete using buildings, highways and other structures have grown by acquiring the land that used to serve as a farming or forest land.

The results obtained from the collection of LST by using Landsat 8 dataset, in ERDAS IMAGINE 2015 software, are given in the form of **Table 5.2**.

Table 5. 2: LST values retrieved from different Landsat 8 images

| Date | Maximum LST (°c) | Minimum LST (°c) | Mean LST (°c) |
|------------|---------------------|---------------------|------------------|
| 01-05-2013 | 41.52 | 27.13 | 35.21 |
| 12-05-2017 | 43.74 | 28.07 | 37.54 |
| 23-05-2021 | 45.46 | 28.14 | 35.35 |

According to the data, the temperature varied between 27.13°C and 41.52°C in 2013, and a average LST of 35.21°C, an overall rise of 2.33°C in average temperature from 2013 to 2017, and increase of 0.14°C in mean temperature from 2013 to 2021. The rise in mean temperature over the last eight years may be linked to an growing in built-up area as well as a decrease in greenery. Also, there is a greater rise in built-up area (up 6.23 percent) and a greater decline in vegetative area (down 8.5 percent) from 2013 to 2017, resulting in a greater increase in average LST from 2017 to 2021. As well as open areas (fallow land), are also reportedly found to have higher temperature which have increased in 2017 from 2013(increased by 2.83%) and decreased in 2021 from 2017 (decreased by 2.98%). After the retrieval of Land surface temperature, it was further studies the variation of LST with various LULC classes, the results of which are given in the table **Table 5.3**.

Table 5. 3: LULC classes and their LST values

| LULC classes | LST 01-05-2013 (°C) | LST 12-05-2017 (°C) | LST 23-05-2021 (°C) |
|--------------|------------------------|------------------------|------------------------|
| Built-up | 35.21 | 36.94 | 35.62 |
| Vegetation | 34.88 | 35.67 | 34.51 |
| Fallow land | 36.75 | 38.38 | 35.20 |
| Sand | 38.32 | 40.63 | 40.84 |
| Water body | 30.00 | 30.40 | 30.51 |

According to the above table, LST exhibits both geographical and temporal fluctuation when the LULC pattern changes. It is also possible to argue that with the increase in urbanization Built-up area, fallow land, or other building activities are also expanding, leading to the growth in LST. Meanwhile, water bodies and plant cover are disappearing, which is also a key role in the rise of LST.

Also, the results of the association among LST and NDVI revealed negative association in locations with higher NDVI values were observed will have lower temperatures than those with low NDVI values. Also, the correlation analysis with LST and NDBI showed the presence of a positive relation in LST with the NDBI that is, as NDBI increases LST also increases.

CHAPTER 6

CONCLUSION

The Land surface temperature model is created in this work which utilizes ERDAS IMAGINE MODEL MAKER to get the LST from the Landsat 8 dataset. This model is compatible with Landsat 8 data. According to the supervised categorization findings, the built-up area has expanded greatly while the green area has dropped dramatically. After studying the LST variance with various LULC classes, it was discovered that an ascending tendency of LST was detected in the majority of the research region where built-up area had expanded. After examining the variance of LST, it became clear the Built-up is among the primary LULC classes responsible for the rise in LST. The correlation research revealed that LST and NDBI have a positive association because solar radiations do not directly touch the surface in built-up areas, and the emissivity is reduced, resulting in greater LST. Correlation study of LST with NDVI reveals a negative trend, indicating that areas with vegetation have lower LST than areas with less vegetation, which have greater LST.

REFERENCES

- [1] Definition of LST. Available online: http://earthobservatory.nasa.gov/GlobalMaps/view.php?d1=MOD11C1_M_LST DA
- [2] A. Rajeshwari and N. Mani, "Estimation of land surface temperature of dindigul district using Landsat 8 data," *International Journal of Research in Engineering and Technology*, vol. 3, no. 5, pp. 122–126, 2014.
- [3] F. Wang, Z. Qin, C. Song, L. Tu, A. Karnieli, and S. Zhao, "An improved mono-window algorithm for land surface temperature retrieval from Landsat 8 thermal infrared sensor data," *Remote Sensing*, vol. 7, no. 4, pp. 4268–4289, 2015.
- [4] J. A. Sobrino, J. C. Jiménez-Muñoz, and L. Paolini, "Land surface temperature retrieval from LANDSAT TM 5," *Remote Sensing of Environment*, vol. 90, no. 4, pp. 434–440, 2004.
- [5] Subhanil Guha, Himanshu Govil, Anindita Dey & Neetu Gill, "Analytical study of land surface temperature with NDVI and NDBI using Landsat 8 OLI and TIRS data in Florence and Naples city, Italy," *European Journal of Remote Sensing*, vol. 51, no. 1, pp. 667-678, 2018.
- [6] Noyingbeni Kikon, Prafull Singh, Sudhir Kumar Singh, Anjana Vyas, "Assessment of urban heat islands (UHI) of Noida City, India using multi-temporal satellite data," *Sustainable Cities and Society*, vol. 22, pp. 19-28, 2016.
- [7] Kaplan, Gordana, Ugur Avdan, and Zehra Yigit Avdan. 2018. "Urban Heat Island Analysis Using the Landsat 8 Satellite Data: A Case Study in Skopje, Macedonia" *Proceedings 2*, vol. 2, no. 7, pp. 358, 2018.
- [8] P. Ramya, V. Sindhura, and P. V. Sagar, "Testing using selenium web driver," 2017 Second International Conference on Electrical, Computer and Communication Technologies (ICECCT), 2017, pp. 1-7, doi: 10.1109/ICECCT.2017.8117878.
- [9] Harpreet Kaur, Dr. Gagan Gupta, "Comparative Study of Automated Testing Tools: Selenium, Quick Test Professional and Test complete" Harpreet kaur et al

Int. Journal of Engineering Research and Applications www.ijera.com ISSN: 2248-9622, Vol. 3, Issue 5, Sep-Oct 2013, pp.1739-1743

- [10] Ruchika Malhotra, "A systematic review of machine learning techniques for software fault prediction" Volume 27, February 2015, Pages 504-518.
- [11] Cagatay Catala, Banu Dirib," A systematic review of software fault prediction studies" Volume 36, Issue 4, May 2009, Pages 7346-7354
- [12] Rathore, S.S., Kumar, S. A study on software fault prediction techniques. *Artif Intell Rev* 51, 255–327 (2019). <https://doi.org/10.1007/s10462-017-9563-5>
- [13] D. M. Powers, "Evaluation: from precision, recall and F-measure to ROC, informedness, markedness and correlation," *Journal of Machine*, 2011.
- [14] Mauricio A. Valle & Gonzalo A. Ruz (2015) Turnover Prediction in a Call Center: Behavioral Evidence of Loss Aversion using Random Forest and Naïve Bayes Algorithms, *Applied Artificial Intelligence*, 29:9, 923-942, DOI: 10.1080/08839513.2015.1082282.
- [15] International Conference on Advances in Computing, Communication Control and Networking (ICACCCN)269 "Predicting Employee Attrition along with Identifying High Risk Employees using Big Data and Machine Learning" , Apurva Mhatre, Avantika Mahalingam, Mahadevan Narayanan, Akash Nair, Suyash Jaju.
- [16] Lessmann, Stefan, and Stefan Voß. "A reference model for customercentric data mining with support vector machines." *European Journal of Operational Research* 199.2 (2009): 520-530.
- [17] T. Fawcett, "An introduction to ROC analysis," *Pattern Recognition Letters* 27), 861–874, 2006.
- [18] A New Multi-layer Perceptrons Trainer Based on Ant Lion Optimization Algorithm Raschka, S. (2015). *Python machine learning*. Packt Publishing Ltd.
- [19] Morgan, J.N., Sonquist, J.A.: Problems in the analysis of survey data, and a proposal. *J. Am. Stat. Assoc.* 58, 415–434 (1963)
- [20] <https://www.upgrad.com/blog/cross-validation-in-python/>
- [21] Géron, A.: *Hands-on machine learning with Scikit-Learn and TensorFlow: concepts, tools, and techniques to build intelligent systems*. O'Reilly Media(2017)
- [22] Ugur Avdan and Gordana Jovanovska. "Automated Mapping of Land Surface Temperature Using LANDSAT 8 Satellite Data", *Journal of Sensors*, Vol. 2016, Article ID 1480307, 2016.

- [23] D. Jeevalakshmi, S. Narayana Reddy, & B. Manikiam. "Land cover classification based on NDVI using LANDSAT8 time series: A case study Tirupati region", IEEE International Conference on Communication and Signal Processing (ICCSP), pp.1332-1335,doi:0.1109/ICCSP.2016.7754369, 2016.
- [24] Javed Mallick, Yogesh Kant, & B.D.Bharath. "Estimation of Land Surface Temperature over Delhi Using Landsat-7 ETM+", J. Ind. Geophys. Union, Vol.12, No.3, pp.131-140, 2008.
- [25] M. Stathopoulou, & C. Cartalis. "Daytime urban heat islands from Landsat ETM+ and Corine land cover data: An application to major cities in Greece", Solar Energy, Vol. 81, no. 3, pp. 358 – 368, 2007.
- [26] Artis, D. A. and Carnahan, "Survey of emissivity variability in thermography of urban areas," Remote Sensing of Environment, vol. 12, no. 4, pp. 313-329.
- [27] Liu, Lin, and Yuanzhi Zhang, "Urban Heat Island Analysis Using the Landsat TM Data and ASTER Data: A Case Study in Hong Kong," Remote Sensing, vol. 3, no. 7, pp. 1535-1552, 2011.
- [28] Xiong, Yongzhu, Shaopeng Huang, Feng Chen, Hong Ye, Cuiping Wang, and Changbai Zhu. 2012. "The Impacts of Rapid Urbanization on the Thermal Environment: A Remote Sensing Study of Guangzhou, South China," Remote Sensing, vol. 4, no. 7, pp. 2033-2056, 2012.